Observing climate I: surface temperatures

John Remedios

Earth Observation Science and NCEO
Dept. of Physics and Astronomy
U. Leicester

Outline

- The Big Picture for Surface Temperature (ST) observations
- General theory of ST remote sensing
- Instruments
- Sea Surface Temperatures
- Land Surface Temperatures
- For the future

Acknowledgements:

David Llewellyn-Jones P.I. (Leicester) and Chris Mutlow (RAL)

The Leicester ATSR team, particularly Karen Veal, Darren Ghent and Gary Corlett (Validation Scientist)

Chris Merchant (Reading) and the ARC team

Research carried out at the Universities of Leicester, Edinburgh, RAL, Oxford, Southampton, Swansea and the Met Office,

Funding: NERC, NCEO and DECC in the UK; ESA, EUMETSAT and Copernicus

The Big Picture

IPCC figures from Chapter 2; WG I report 2013

Hartmann, D.L., A.M.G. Klein Tank, M. Rusticucci, L.V. Alexander, S. Brönnimann, Y. Charabi, F.J. Dentener, E.J. Dlugokencky, D.R. Easterling, A. Kaplan, B.J. Soden, P.W. Thorne, M. Wild and P.M. Zhai, 2013: Observations: Atmosphere and Surface. In: Climate Change 2013: The Physical Science Basis. Contribution of Working Group I to the Fifth Assessment Report of the Intergovernmental Panel on Climate Change [Stocker, T.F., D. Qin, G.-K. Plattner, M. Tignor, S.K. Allen, J. Boschung, A. Nauels, Y. Xia, V. Bex and P.M. Midgley (eds.)]. Cambridge University Press, Cambridge, United Kingdom and New York, NY, USA, pp. 159–254, doi:10.1017/CBO9781107415324.008.

Planetary Warming

Very well known:

- Surface temperature (ST) has changed over last century (~0.9 K 1901-2012)
- Records are driven by in situ historical records for much of the century. Independent observations have been lacking.
- Recent observed temperature change and prediction of decadal change will be a key focus for next few years of research (recent change has been of order 0.05 K/decade or less).
- IPCC 5th Assessment, Working Group I report, has just been released. There is clearly a better understanding of uncertainties and biases in the ST record.

IPCC: Land Surface Air Temp

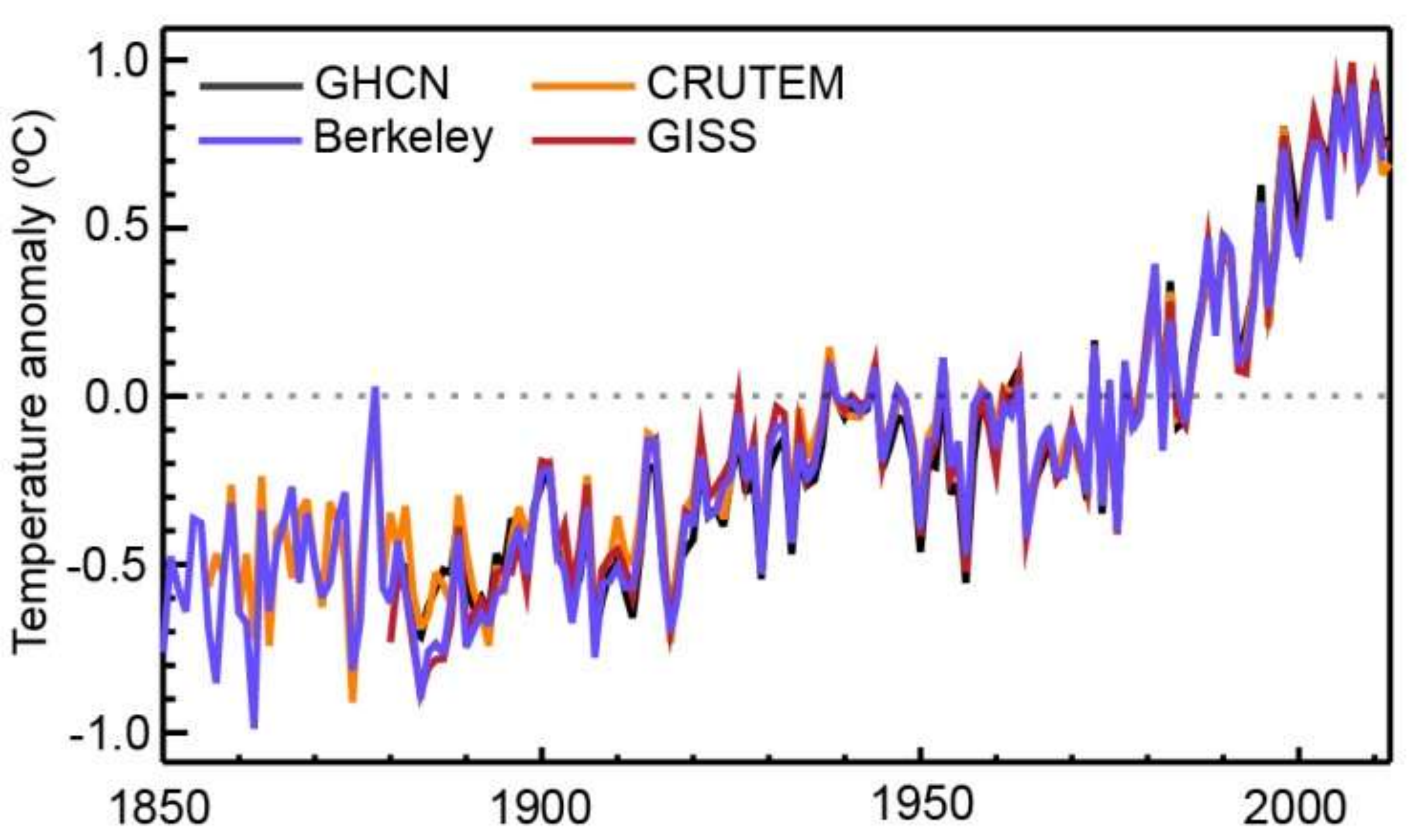

Figure 2.14: Global annual average Land-Surface Air Temperature (LSAT) anomalies relative to a 1961–1990 climatology from the latest versions of four different datasets (Berkeley, CRUTEM, GHCN and GISS).

IPCC: Sea Surface/Marine Air Temp

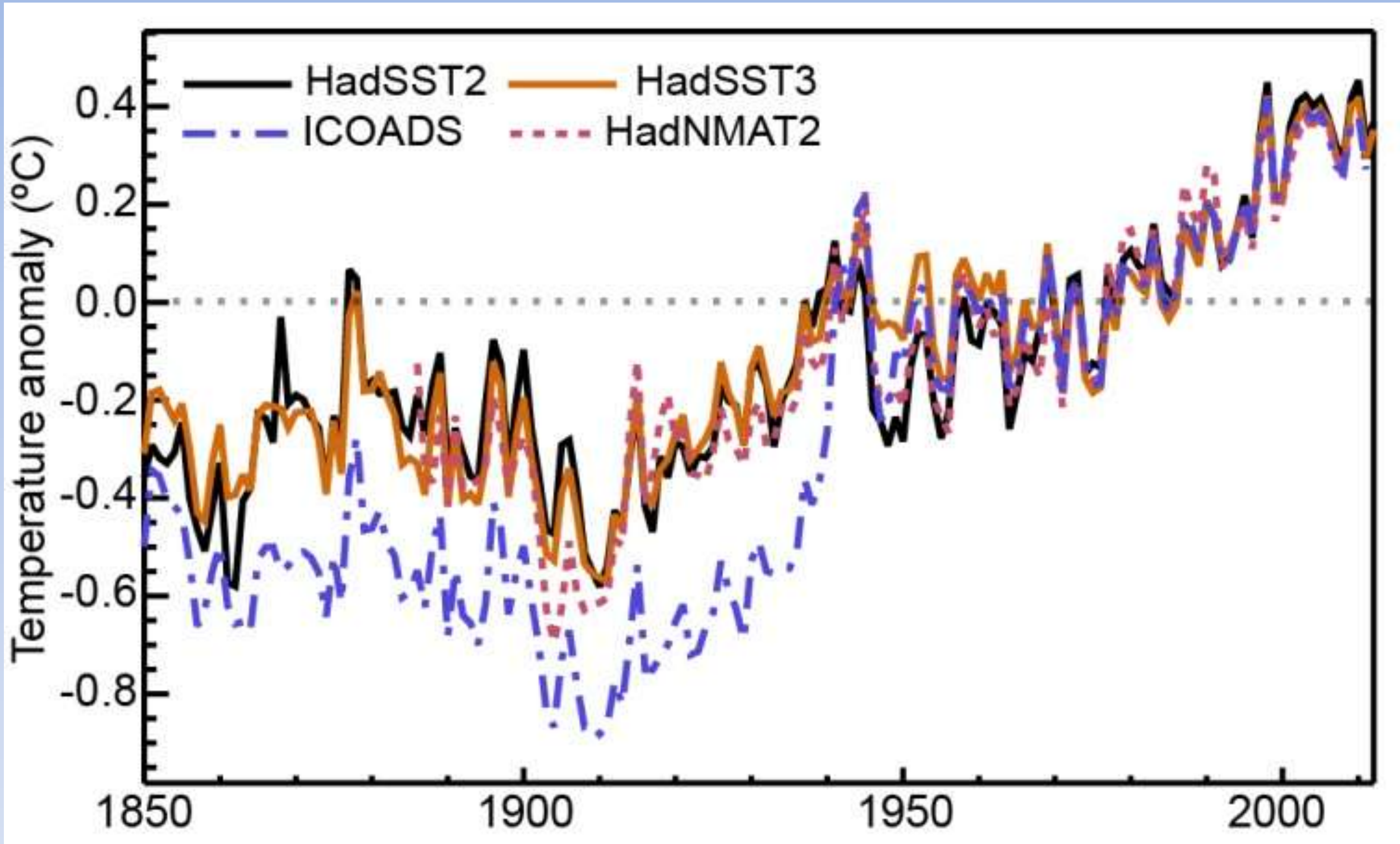

Figure 2.16: Global annual average Sea Surface Temperature (SST) and Night Marine Air Temperature (NMAT) relative to a 1961–1990 climatology from gridded datasets of SST observations (HadSST2 and its successor HadSST3), the raw SST measurement archive (ICOADS, v2.5) and night marine air temperatures dataset HadNMAT2 (Kent et al., 2013). HadSST2 and HadSST3 both are based on SST observations from versions of the ICOADS dataset, but differ in degree of measurement bias correction.

IPCC: Changing in situ records

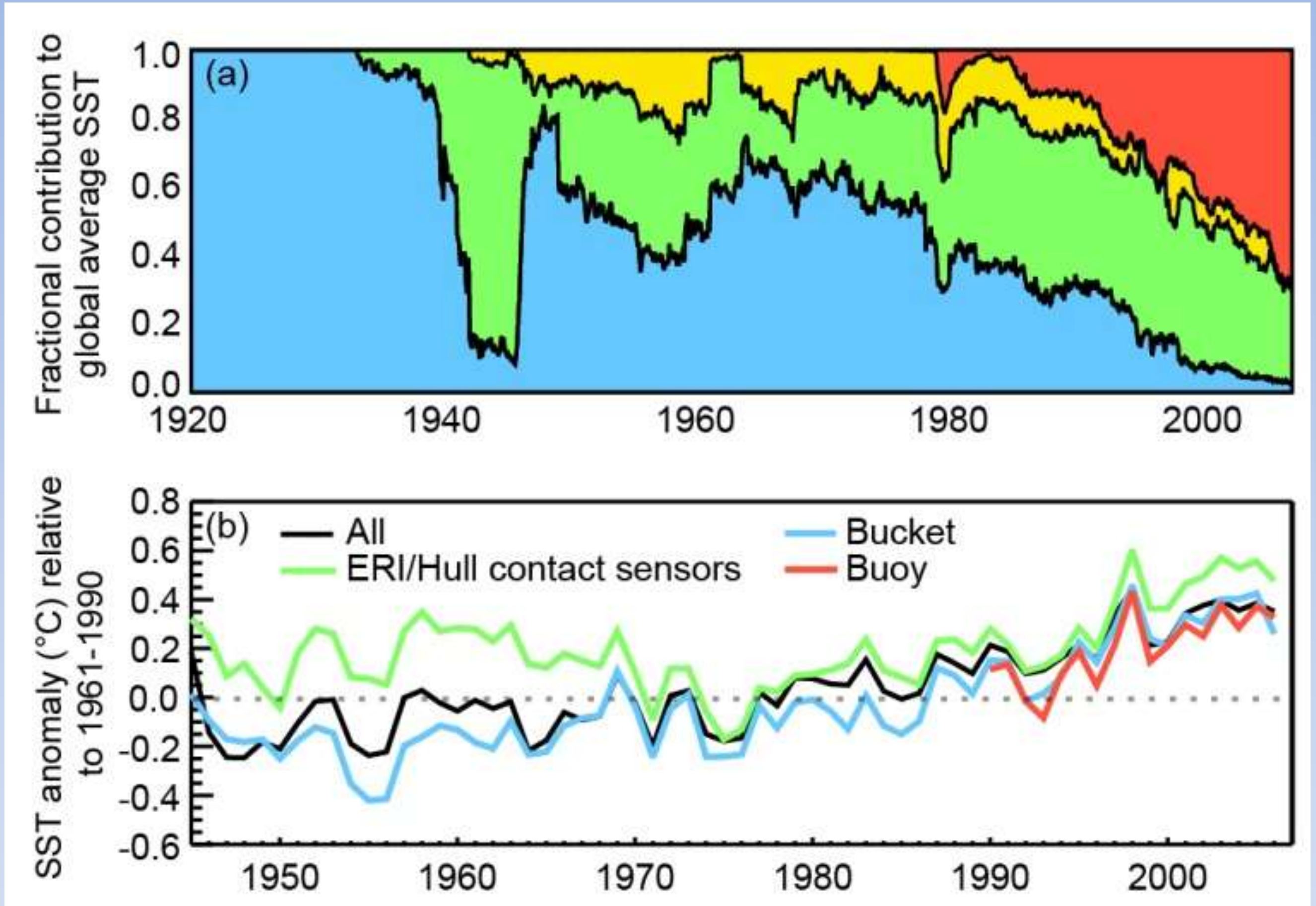

Figure 2.15: Temporal changes in the prevalence of different measurement methods in the International Comprehensive Ocean-Atmosphere Dataset (ICOADS). a) fractional contributions of observations made by differen measurement methods: bucket observations (blue), engine room intake (ERI) and hull contact sensor observations (green), moored and drifting buoys (red), and unknown (yellow). b) Global annual average Sea Surface Temperature (SST) anomalies based on different kinds of data: ERI and hull contact sensor (green), bucket (blue), buoy (red), and all (black). Averages are computed over all 5° ? 5° where both ERI/hull and bucket measurements, but not necessarily buoy data, were available. Adapted from Kennedy et al. (2011a).

IPCC: Integrated (full grid) SST

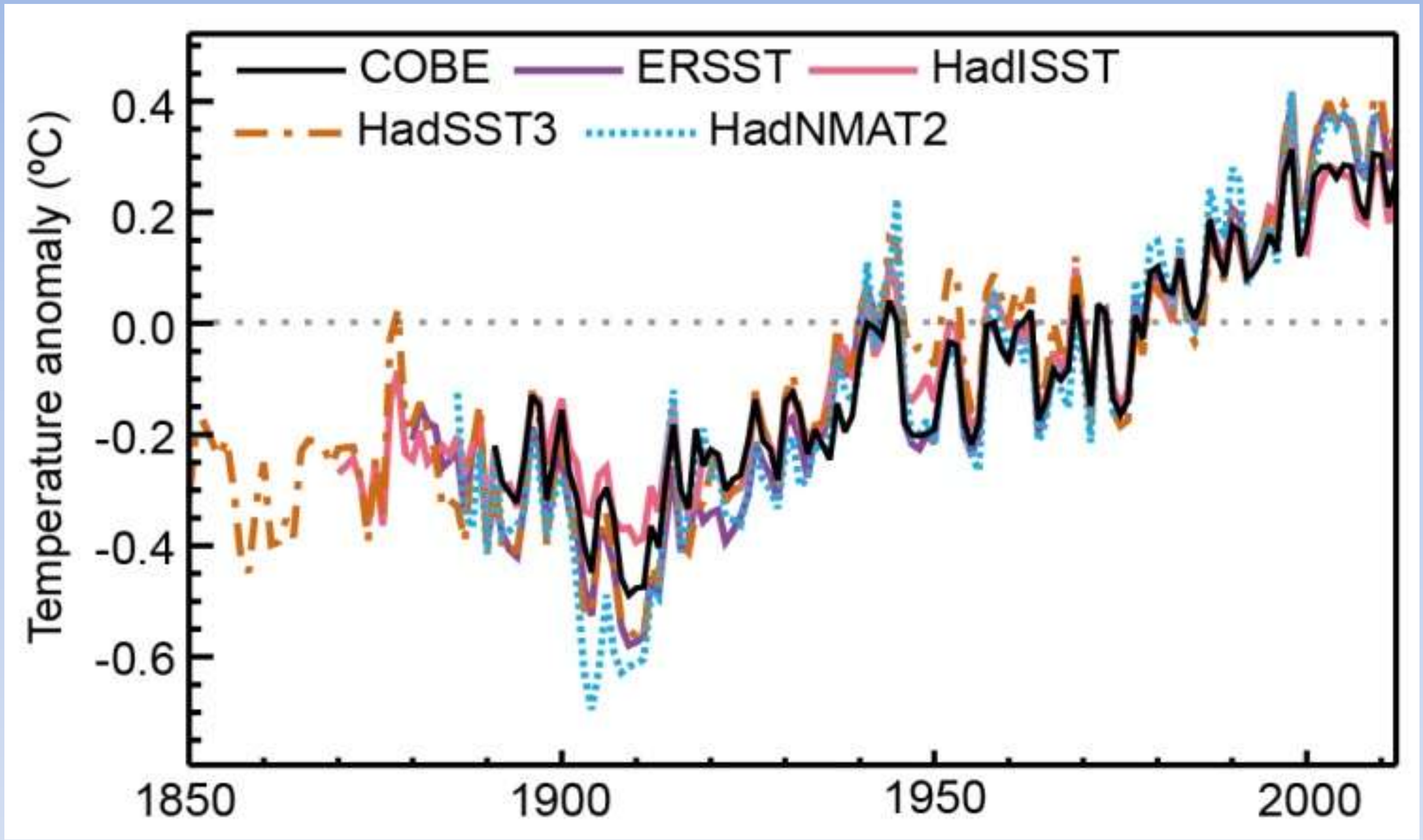

Figure 2.18: Global annual average Sea Surface Temperature (SST) and Night Marine Air Temperature (NMAT) relative to a 1961–1990 climatology from state of the art datasets. Spatially interpolated products are shown by solid lines; non-interpolated products by dashed lines.

General Theory of Surface Temperature Remote Sensing

University of Leicester

The Planck function

EOS

- In order to measure temperature we need a property of a material that is highly sensitive to it.
- Planck, "the reluctant revolutionary", provided in 1900 (approx.) the formula we need to show this sensitivity, and at the same time relates it to energy flux.
- The formular became known as the Planck function for blackbody radiation (isotropic radiator of emissivity 1.0):

$$B(\lambda,T)\ d\lambda = \frac{2hc^2}{\lambda^5\{\exp(hc / k\lambda T) - 1\}}\, d\lambda$$

The equation holds for surfaces and atmospheres in local thermodynamic equilibrium

- It gives the emergent flux emitted from a body at fixed temperature T per unit area, solid angle and per spectral unit (in this case wavelength or λ).
- k is Boltzmann's constant, c is speed of light, and h is Plancks's constant
- We can build blackbodies at Earth temperatures – vital for calibration.

Nobel Prize for Physics (1918): "Discovery of Energy quanta"

AATSR ENVISAT G-STEP

The Earth emitted radiation

The Earth radiates energy because it has a temperature (300 K), just like the sun (6000 K) emits in the visible. We can observe this in spectra recorded by satellites at Top of atmosphere (TOA).

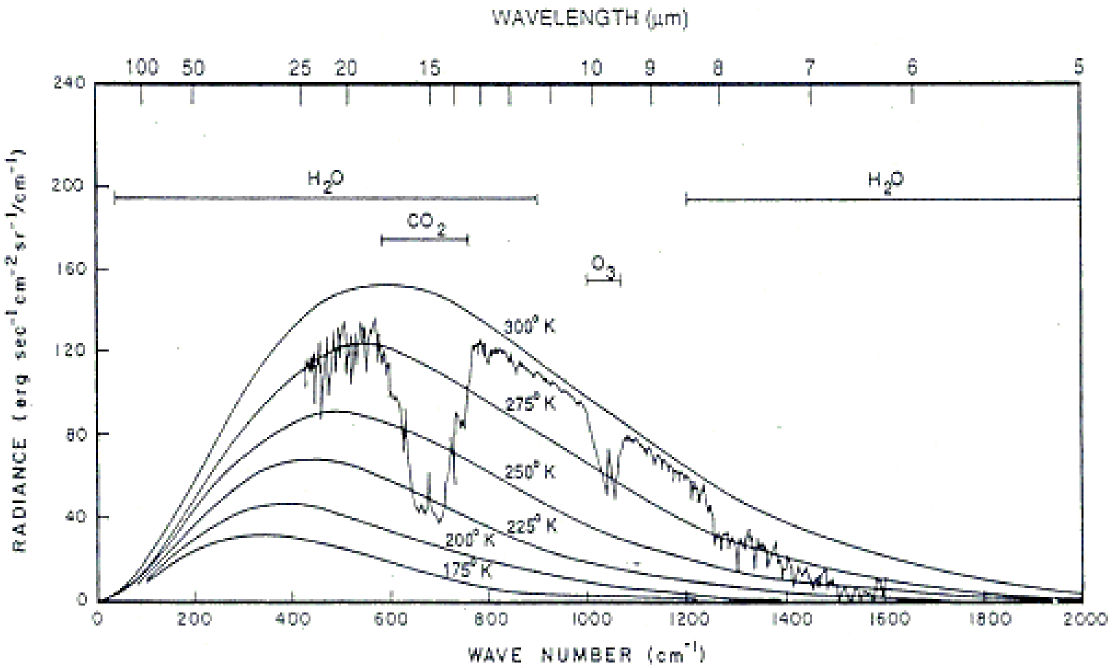

Figure 8.5 Spectrum of outgoing LW radiation over (215° W, 15° N) observed by Nimbus-4 IRIS, as a function of wavenumber λ^{-1}. Blackbody spectra for different temperatures and individual absorbing species indicated. Adapted from Liou (1980).

Planck function shows that the emitted energy peaks between 15 and 20 μm: the thermal infra-red! TOA spectra are clearly modified Planck curves.

The infra-red (emission) spectrum

Wavenumber = 1/ λ but in cm^{-1}. Ref. pt. 10 μm = 1000 cm^{-1}

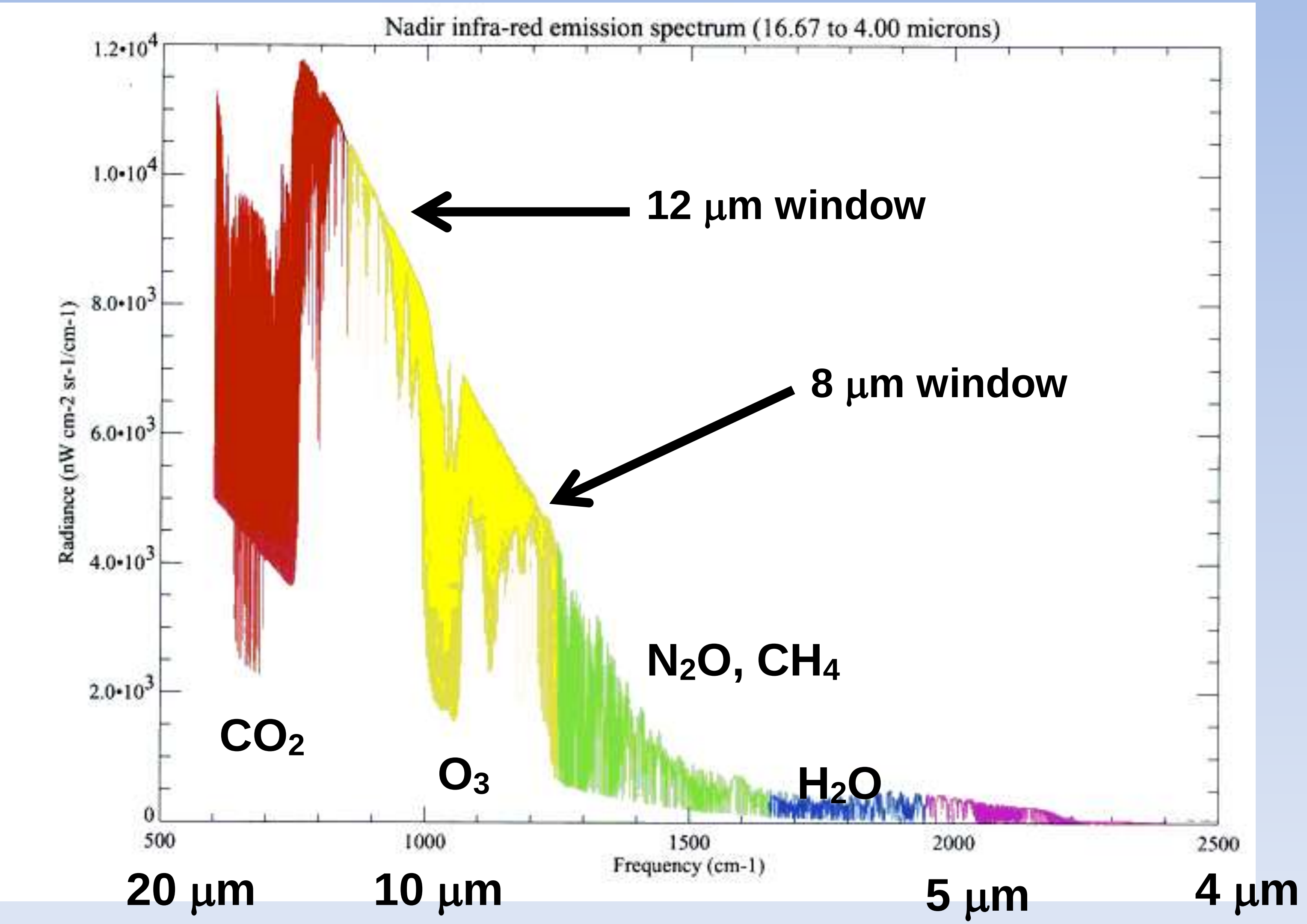

[Nadir simulated signal for an infra-red instrument]

11, 12 micron (ATSR) Spectral Response Functions

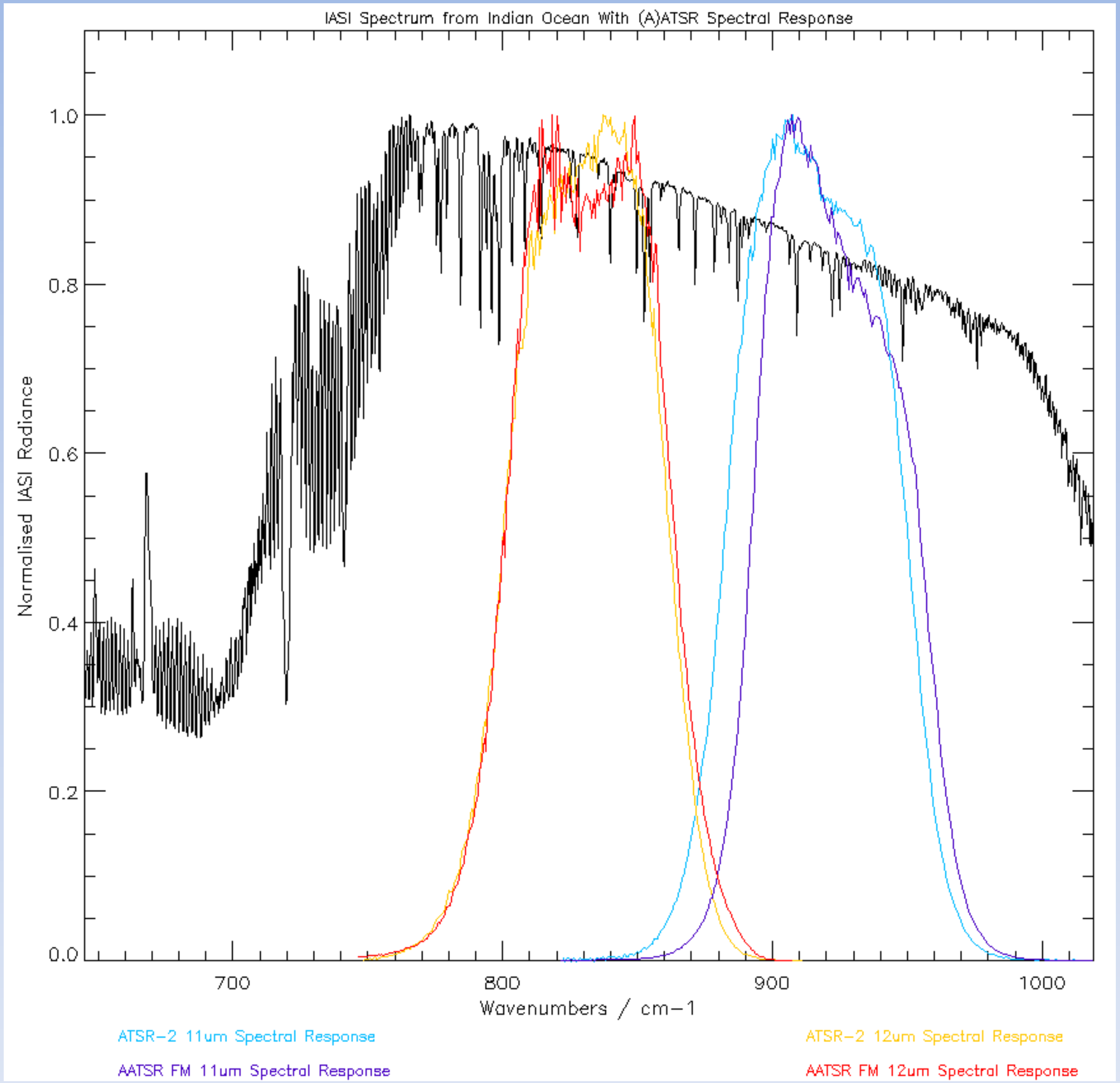

Thermal emission part of the outgoing spectrum is driven by temperature

ATSR spectral functions overlaid on typical IASI spectrum.

AATSR spectral filters are "pre-flight"

Both ATSR-2 and AATSR filter functions are shown

The microwave spectrum

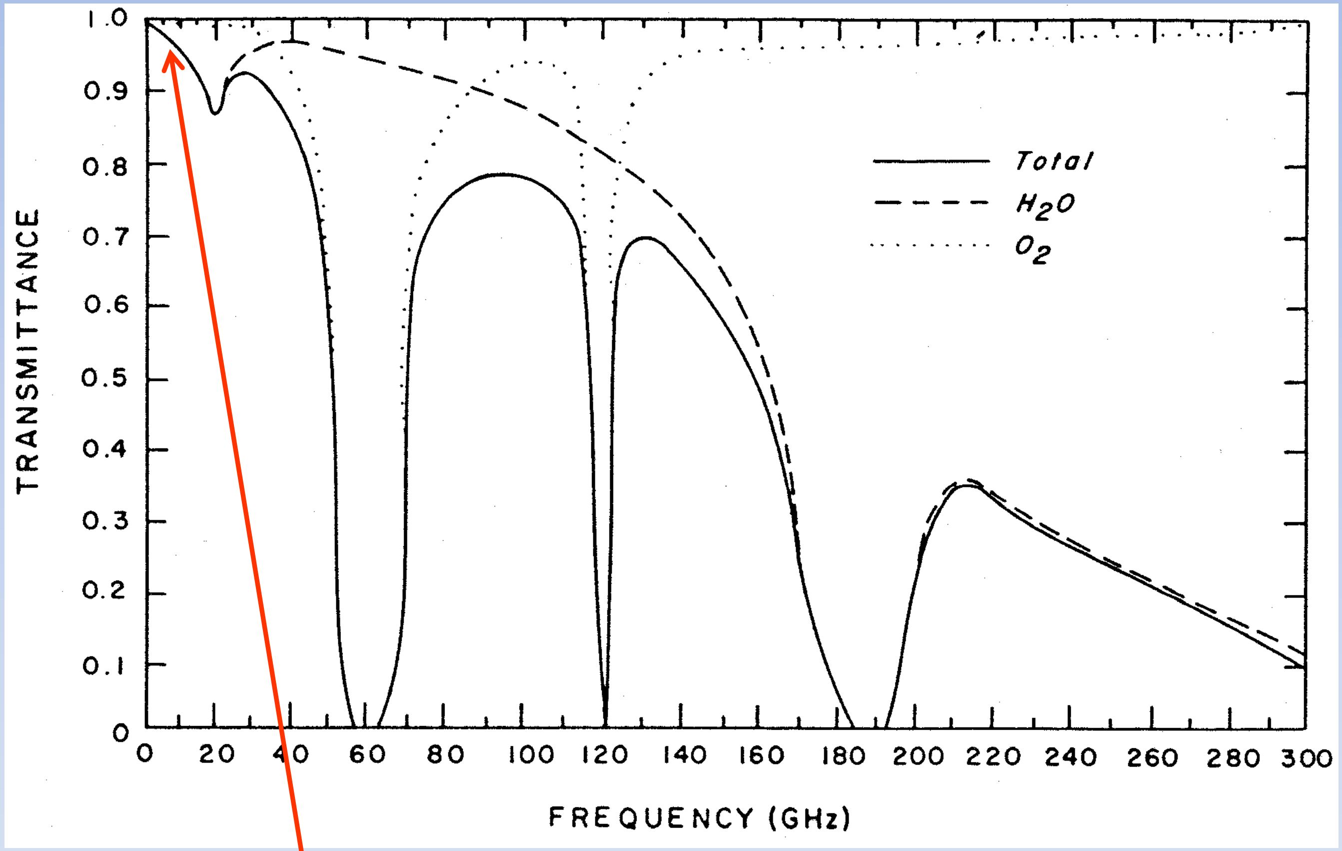

6.9 GHz, 10.7 GHz; avoid interfering signals etc.

Surface temperature : a simple radiative transfer equation

$$L_i^{TOA} = B_i(T_i) = \left[\varepsilon_i B_i(T_s) + (1-\varepsilon_i) L_i^{\downarrow}\right]\tau_i + L_i^{\uparrow}$$

Radiance L measured in channel i (centre wavelength λ(i))

Surface emissivity, ε; 2nd term is reflectance

Atmospheric effects

- Radiance is the power emitted per unit area per unit solid angle; TOA is top of atmosphere. Ti is the equivalent temperature whose Planck function=radiance
- The arrows refer to the downwelling and upwelling components of atmospheric radiance contributions
- ε is the emissivity of the surface with temperature Ts.
- These equations hold for channels, i, e.g. radiometers, but also at each wavelength of the spectrum.
- τ is the atmospheric transmission of channel i

- Two typical channels, say 11 and 12 microns

$$B_{11}(T_{11}) = \left[\varepsilon_{11} B_{11}(T_s) + (1-\varepsilon_{11}) L_{11}^{\downarrow}\right]\tau_{11} + L_{11}^{\uparrow}$$

$$B_{12}(T_{12}) = \left[\varepsilon_{12} B_{12}(T_s) + (1-\varepsilon_{12}) L_{12}^{\downarrow}\right]\tau_{12} + L_{12}^{\uparrow}$$

- Crucial aspects are $\varepsilon_{11} \approx \varepsilon_{12}$ but they are different. Similarly, L_{11} different to L_{12}
- Generally (but not always) the downwelling terms are small ($\varepsilon_{11} \approx 1.0$)
- τ is close to unity but significant in the tropics and with clouds and aerosols.
- Channels between 3.5 and 4.0 microns are also useful at night (no solar contamination).
- Approximations provide split-window solution; ST related to BTs

$$ST = a_{f,i,pw} + b_{f,i}(T_{11} - T_{12})^{p(\theta)} + (b_{f,i} + c_{f,i})\, T_{12}$$

Thermal infra-red sea emissivity

Ideally, surface emissivity should be unity (or close to), invariant with sea surface state and with a known dependence (if any) on wavelength

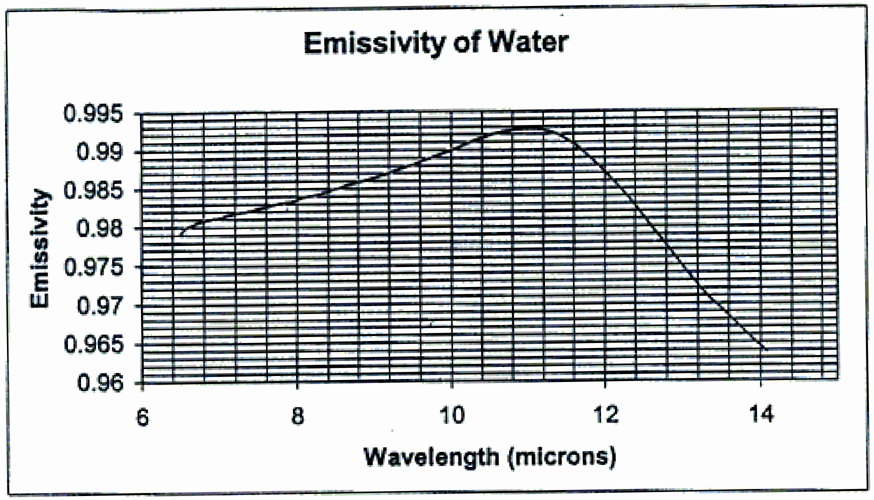

Figure 58: Graph of the emissivity of water as a function of wavelength (following Sidran, 1981)

ε **Variation with λ** near 10 μm.

Infra-red ε depends to a small degree on temperature and sea slope distributions

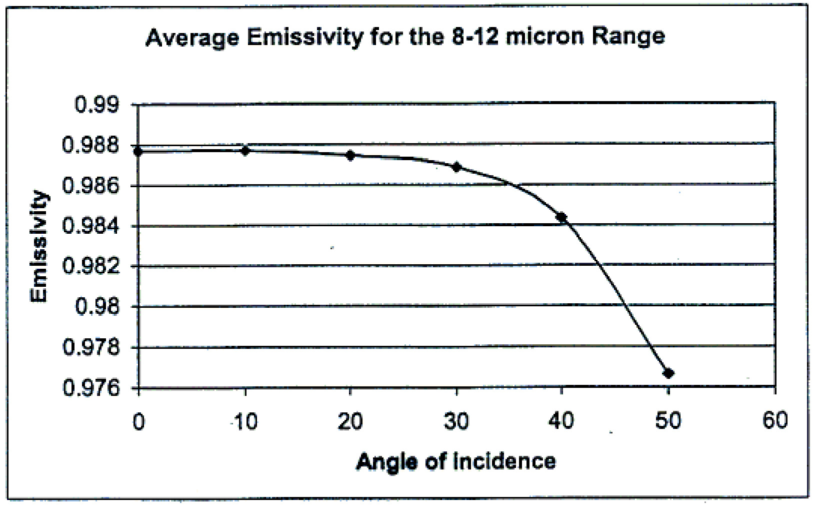

Figure 59: Graph showing the variation of emissivity with viewing angle (from nadir) for the 8-12μm region.

ε **Variation with angle** near 10 μm.

Microwave emissivity

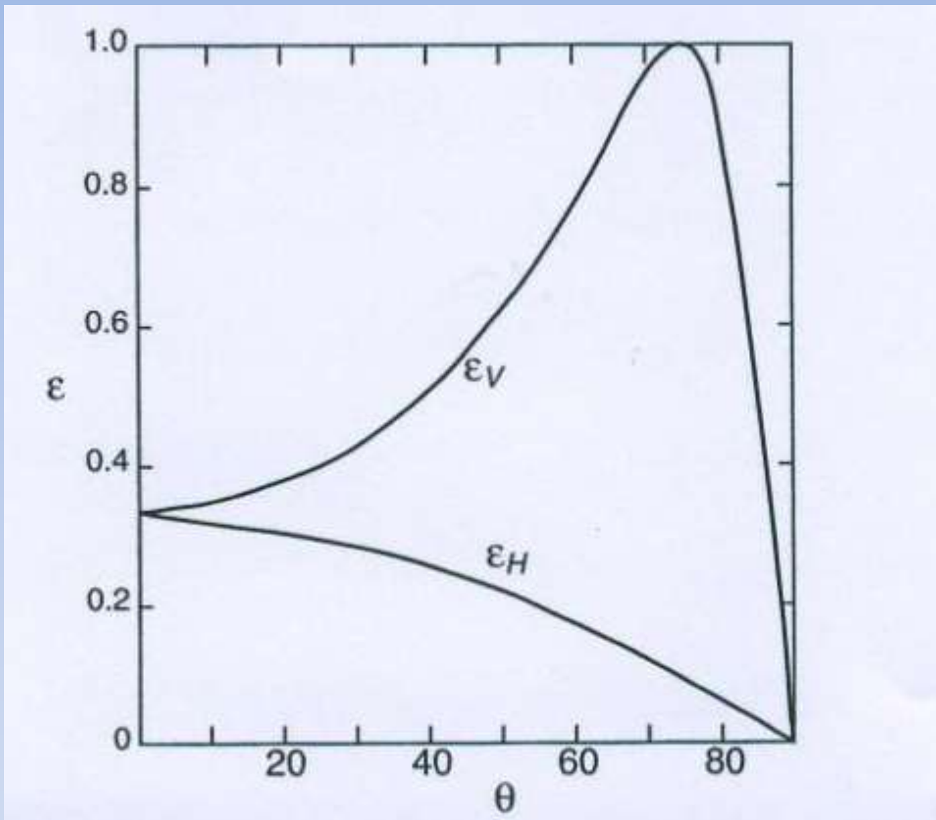

ε **viewing angle variation**: horizontally and vertically polarised emissivity (typical microwave). (I.S. Robinson)

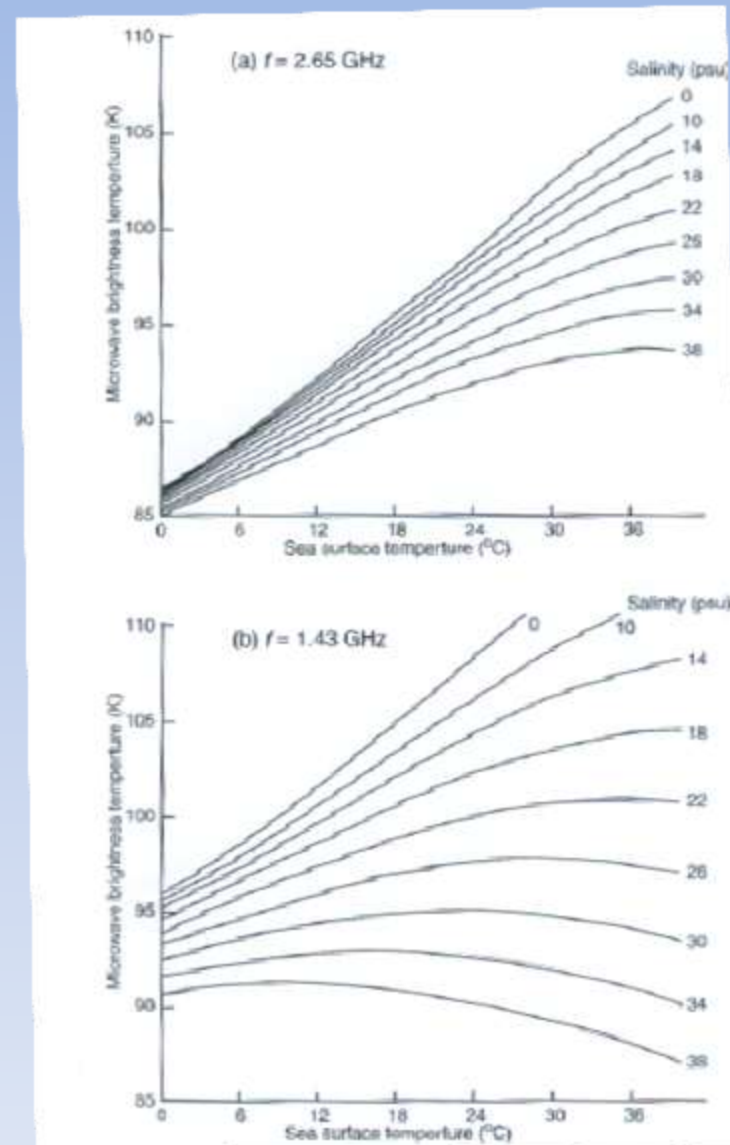

BT variation with SST and salinity. Implication is emissivity varies with salinity! (I.S. Robinson)

Land surface Emissivity

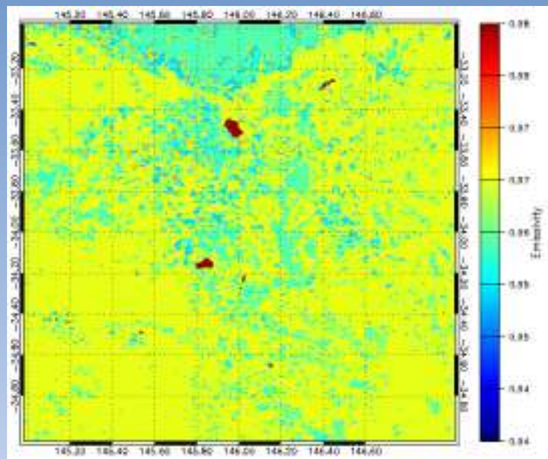

Emissivity 11μm channel

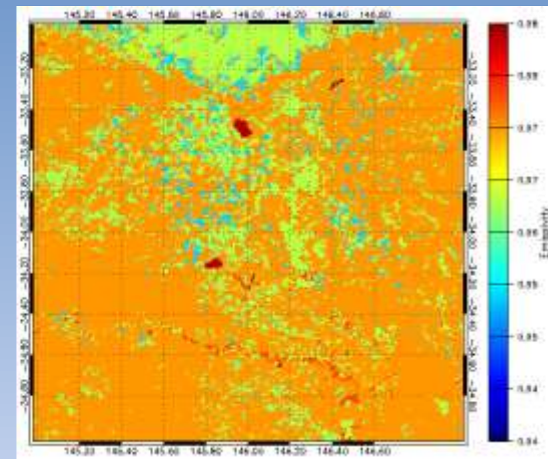

Emissivity 12μm channel

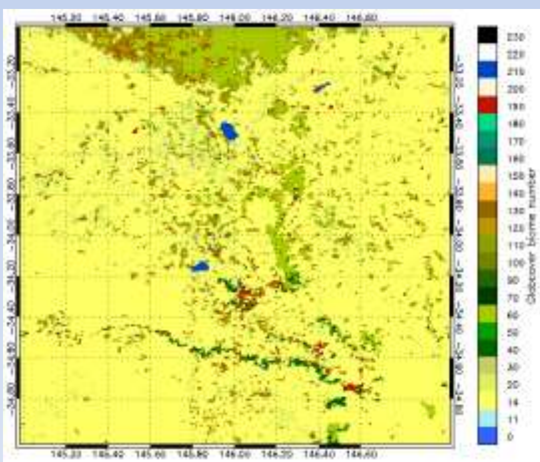

Biome - Globcover

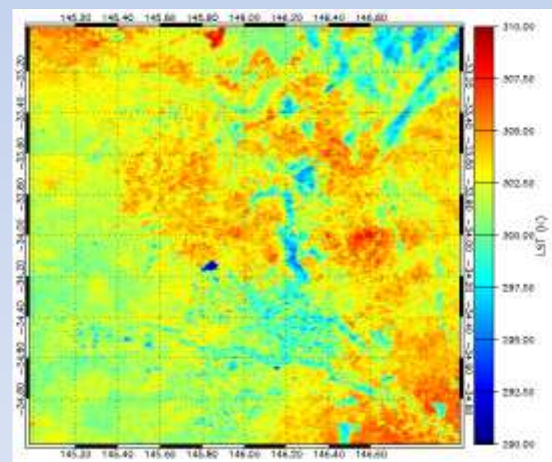

LST

D. Ghent

Atmosphere correction

- Use atmospheric windows where atmospheric transmission is close to unity, e.g., 10-13 μm and 8-9 μm.
- Use multiple channels to give differential sensitivity to surface and atmosphere
- Use more than one view of the same surface pixel to give better atmosphere correction (ATSR dual-view)
- Use physical radiative transfer modelling or regression to account for residual atmosphere variations.
- Require channels and techniques for cloud detection (thermal infra-red), and rainfall (microwave).
- For thermal infra-red instruments, may also need corrections for aerosols in stratosphere and troposphere.

Instruments and calibration

I/R Instruments

AATSR

- ENVISAT, Polar Orbiting
- Sun-Synchronous (~10.00a.m. descending)
- Launched 2001, EOL 2014
- Mission Series (ATSR-1 and ATSR-2) has been operational since 1991
- LST derived from TIR channels: 11 and 12μm
- High Spatial Resolution (1km^2) and Global Coverage
- Narrow swath width (512km)

AVHRR

- NOAA + METOP, Polar Orbiting
- Sun-Synchronous (a.m. descending)
- Mission Series stretching back over 20 years
- LST derived from TIR channels: 11 and 12μm
- High Spatial Resolution (1km^2) and Global Coverage
- Wide swath width (~2500km)

MODIS

- 2 Polar Orbiting satellites: Terra and Aqua
- Terra: Sun-Synchronous (~10.30a.m. descending)
  Launched 1999, EOL 2011
- Aqua: Sun-Synchronous (~13.30a.m. descending)
  Launched 2002, EOL 2011
- LST derived from TIR channels: 11 and 12μm
- High Spatial Resolution (1km^2) and Global Coverage
- Wide swath width (2330km)

SEVIRI

- Meteosat9/MSG2
- Geostationary (0° latitude, 0° longitude)
- Launched 2005, EOL 2015
- LST derived from TIR channels: 10.8 and 12μm
- High Temporal Resolution (15mins)
- Lack of Global Coverage
- Poor Spatial Resolution: 3km at nadir; +6km above 60°

N.B. Also microwave for SST

A climate SST record

- A long-time series of well-calibrated instruments
- Overlap between instruments in series
- Ability (ideally) to validate SST data
- Uncertainty budget
  - random errors
  - algorithm and alignment errors
  - Sampling errors (temporal and spatial)
- Adequate coverage to compute global time series with low errors
- Ability to compute anomalies with respect to an SST climatology

The ATSR Mission

- The Along Track Scanning Radiometer (ATSR) Mission
- Primary objective to measure Sea Surface Temperature (SST) with an accuracy of 0.3 K (1-sigma limit)
- Thermal and visible data for land studies (e.g. temperature, vegetation):
    - Secondary objective is to measure Land ST (LST) with an accuracy of 1.0 K at night and 2.5 K during the day (1-sigma limit)
- Provision of a long-term dataset for global climate change studies

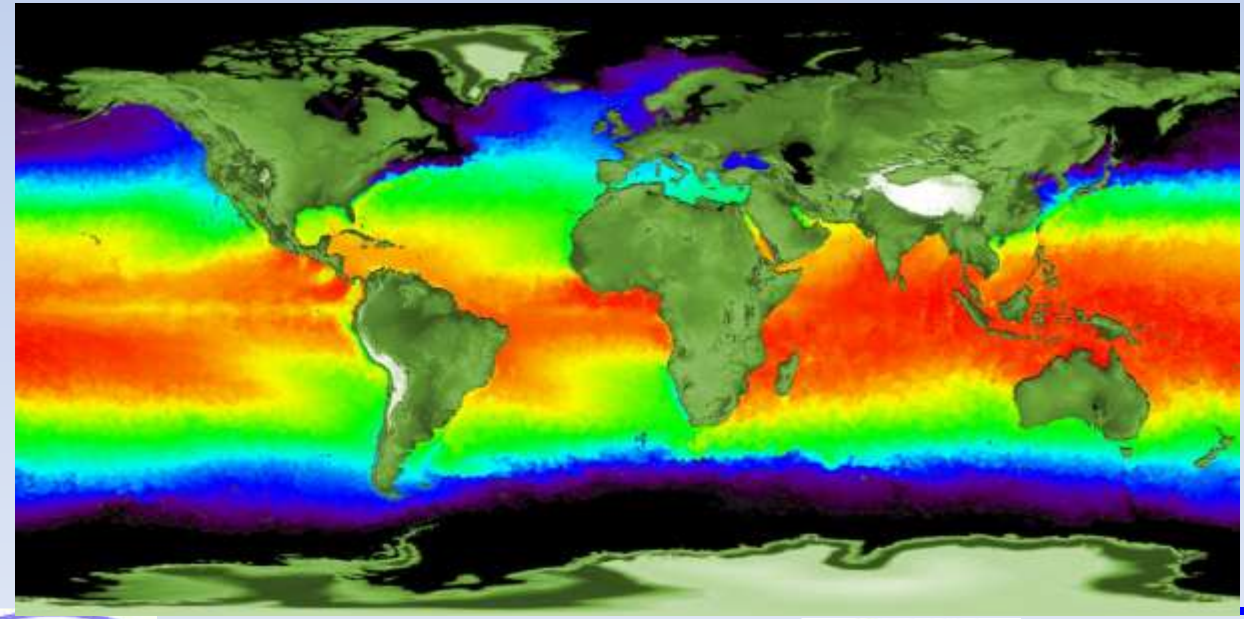

- ATSR-1 (ERS-1) 09/1991 - 03/00
- ATSR-2 (ERS-2) 04/95 - now
- AATSR (Envisat) 03/02 – 04/12
- SLSTR (Sentinel-3)

The Advanced ATSR on ENVISAT

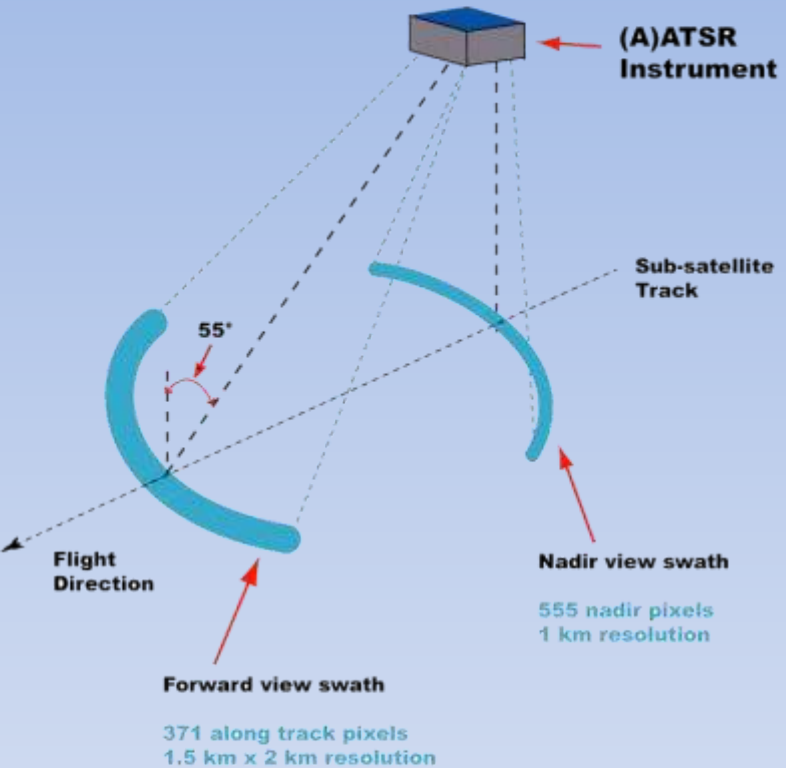

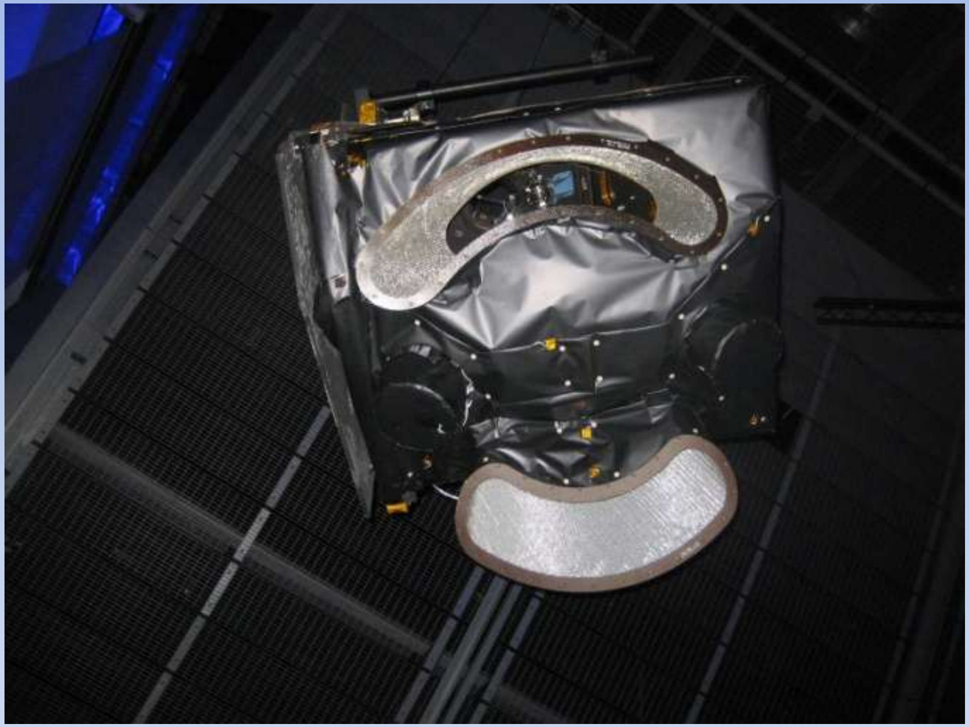

AATSR:

- Dual-view infra-red radiometer (atmosphere correction)
- Three thermal IR channels for surface temperature (ST): 12, 11 and 3.7 microns
- Intrinsic on board calibration: 2 accurate on-board black bodies for IR calibration
- 1 km resolution, 512 km swath width
- Excellent long-term performance in space

BB Temperature Sensor Stability

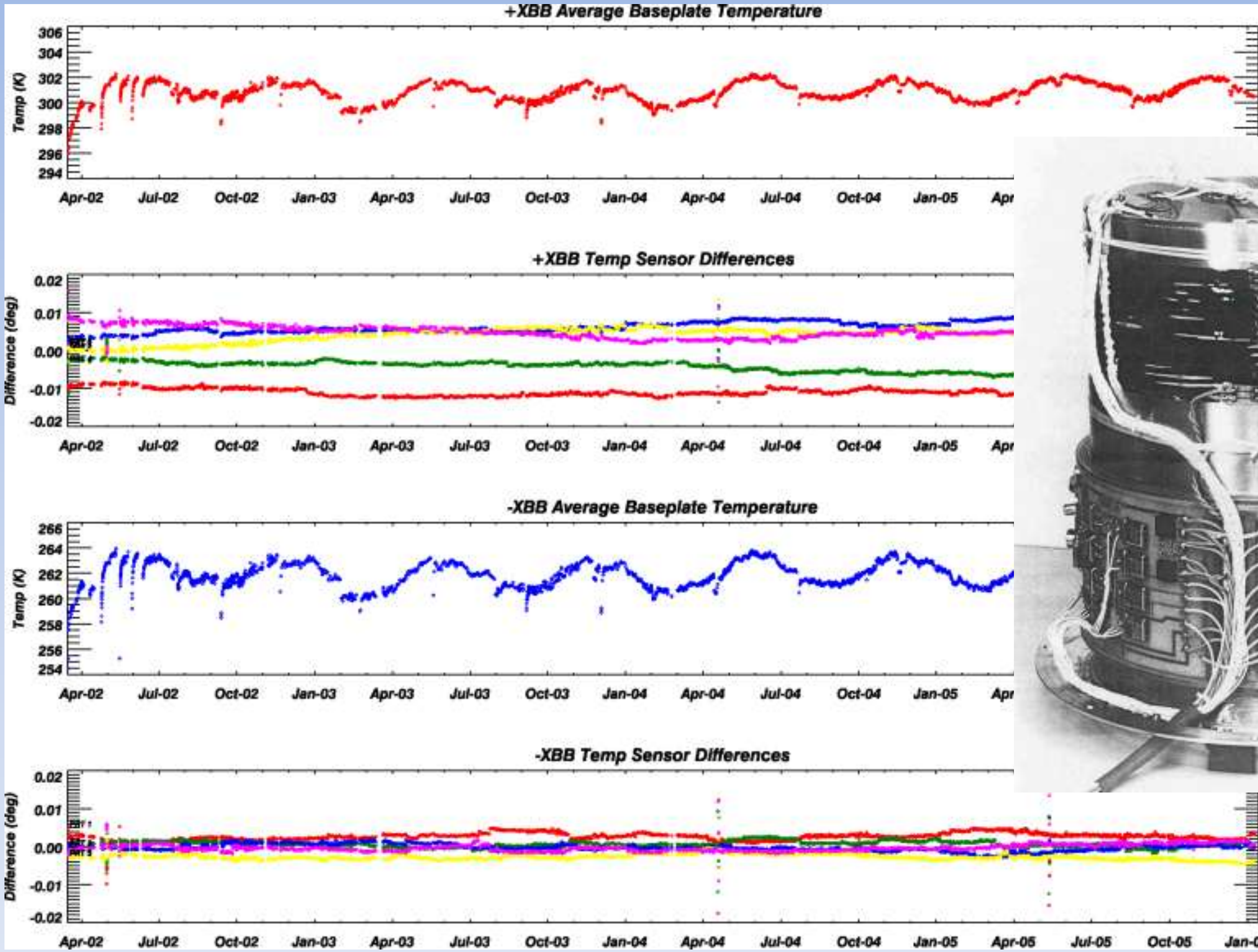

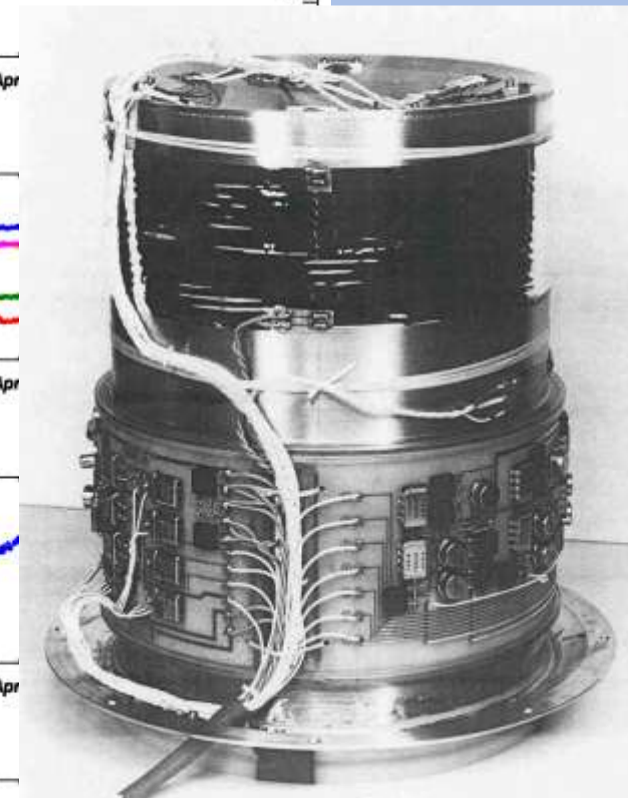

Operational ATSR SST Products

Retrieval	Characteristics	Issues
Night Dual 3 channel D3	**Ultimate retrieval –** Dual view; 3 channel including 3.7 μm.	Clouds – no visible channels
Night Nadir 3 Channel N3	Not dual but still 3.7 μm	Clouds – no vis. channels (but dual-view clouds)
Day Dual 2 Channel D2	Dual view but no 3.7 μm channel	Daytime cloud clearing
[Night Dual 2 channel D2	Dual but no 3.7 μm channel	Clouds – no vis. channels (but dual-view clouds]
Day Nadir 2 Channel N2	The most limited retrieval: no dual, no 3.7 μm	Daytime cloud clearing
[Night Nadir 2 Channel	The most limited retrieval: no dual, no 3.7 μm	Clouds - no vis. channels (but dual-view clouds)]

Validation

- **Two essential validation routes:**
  - Accurate radiometers (direct skin SST measurements; local regions; increasing time series); hundreds to thousands of match-ups
  - Global drifting buoys (much larger nos.; depth measurements); tens of thousands of match-ups

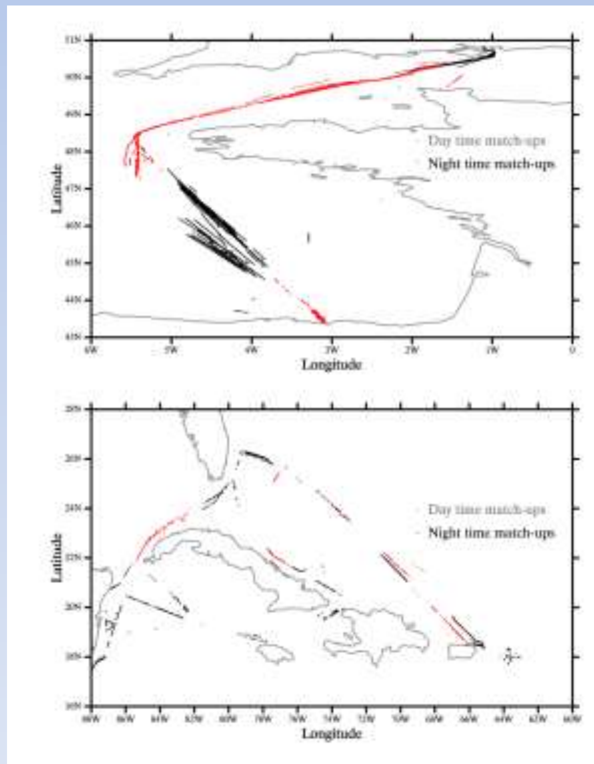

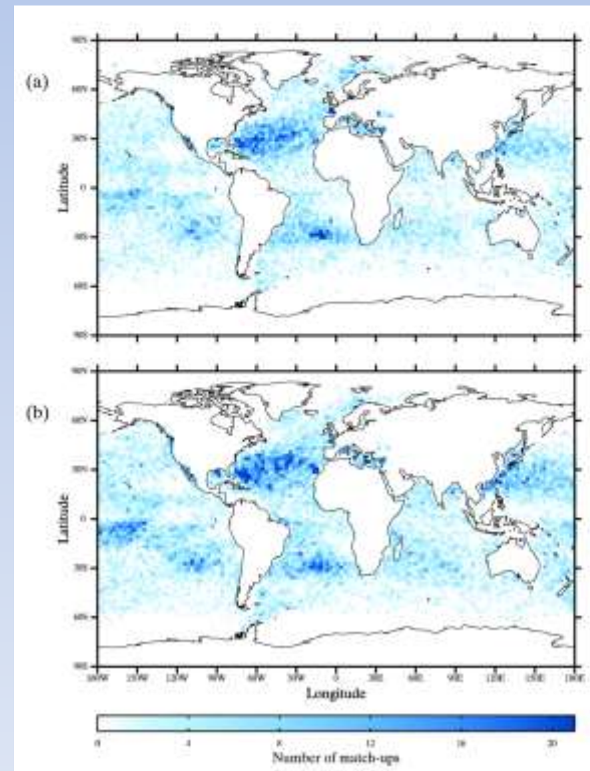

AATSR V2.0 vs IN SITU (G. Corlett)

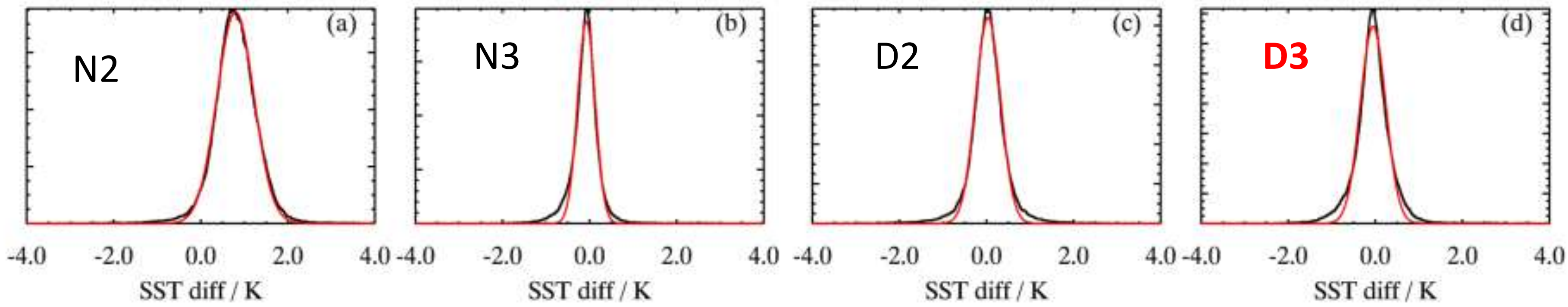

All match-ups limited to wind speeds < 6 ms^{-1}
Median differences (and Gaussian Fit above)
Expect 'constant offset' of -0.17 K from buoys.
Robust statistics (below)

Absolute accuracy of the order of 0.15 K
Very good defn of sd

Retrieval	ISAR					Drifters				
	Number	Nadir-only		Dual-view		Number	Nadir-only		Dual-view	
		Median (K)	RSD (K)	Median (K)	RSD(K)		Median (K)	RSD (K)	Median (K)	RSD (K)
Day time 2-	1193	+0.70	0.46	-0.02	0.44	126	+0.65	0.36	+0.06	0.31
Night time 3-	2352	+0.10	0.18	+0.03	0.27	141	-0.07	0.23	+0.01	0.31

AATSR vs ATSR-2 SST

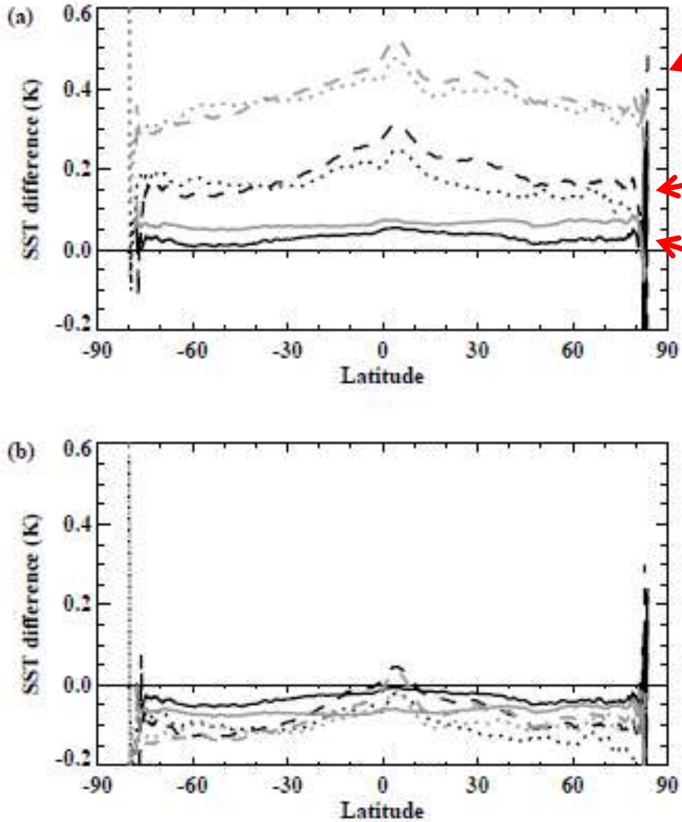

2 channel; nadir

Veal et al, 2013

2 channel; dual

3 channel dual

After 12 micron correction;
Removal of mean bias: +/- 0.03 K for relative error between 2 sensors

Figure 3: The mean difference between the daily average SST of AATSR and ATSR-2 (AATSR minus ATSR-2) is plotted against latitude separately for each retrieval type: (a)without an offset applied to the AATSR 12 μm BT, (b) the AATSR SST has been processed with a constant offset of +0.2 K applied to the 12 μm BTs. Dual-view SSTs are plotted in black, nadir-only SSTs in grey, night-time 3-channel (solid), night-time 2-channel (dashed) and day-time 2-channel (dotted).

In-flight verification: AATSR vs IASI BTs

- **AATSR vs ATSR-2 showed ~0.2 K difference at 12 μm BT; much less at 11 μm**
- **We can verify by comparising IASI spectral measurements for ATSR radiometry**
- **New intercomparisons of AATSR and IASI show T-dependent bias at 12 microns (detector non-linearity; wavelength shift)**

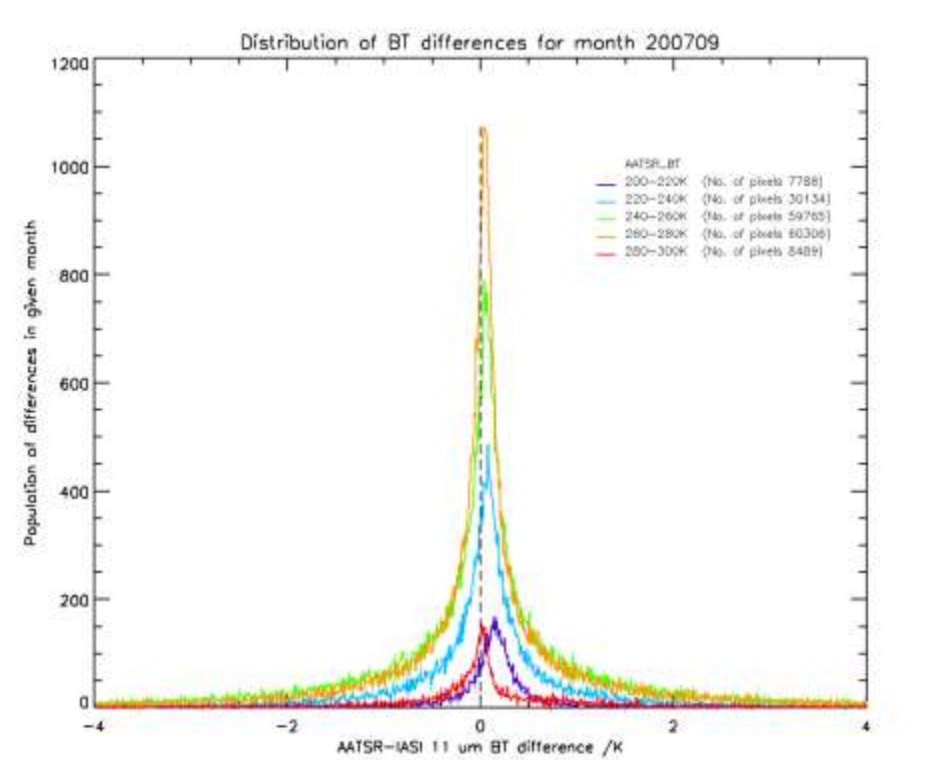

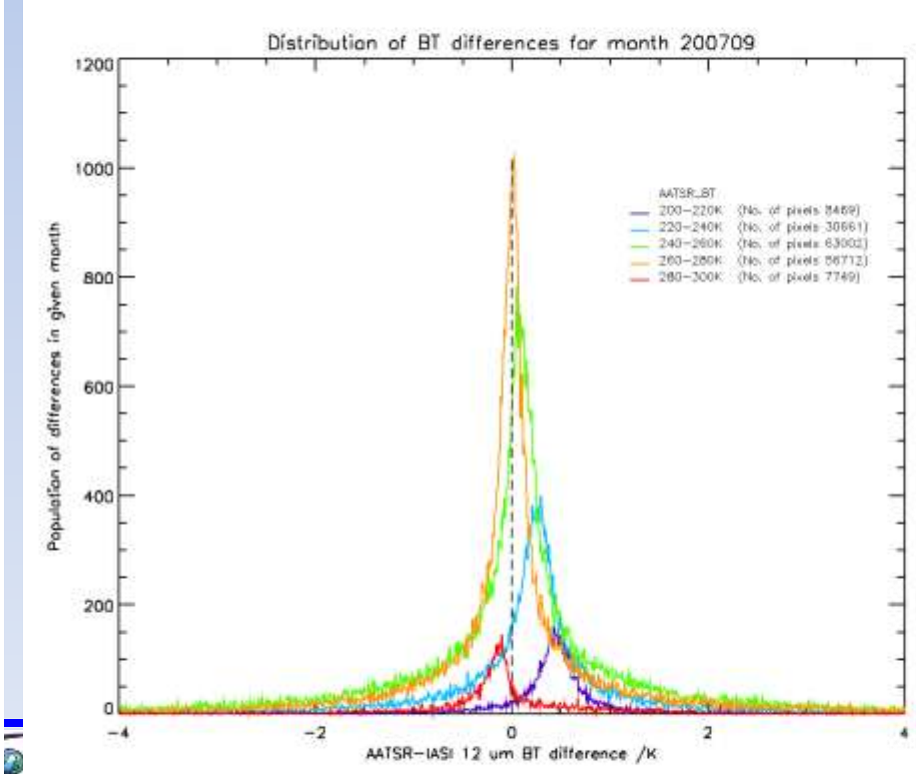

ATSR SST time series

SST time series

- A gridded climatology
- A gridded data set at good spatial resolution (10 arc min; approx. 15 km)
- A monthly SST data set with continuous time series at as many grid points as possible (5° grid boxes)
- A means to estimate uncertainty

ATSR SST data for 1 day.

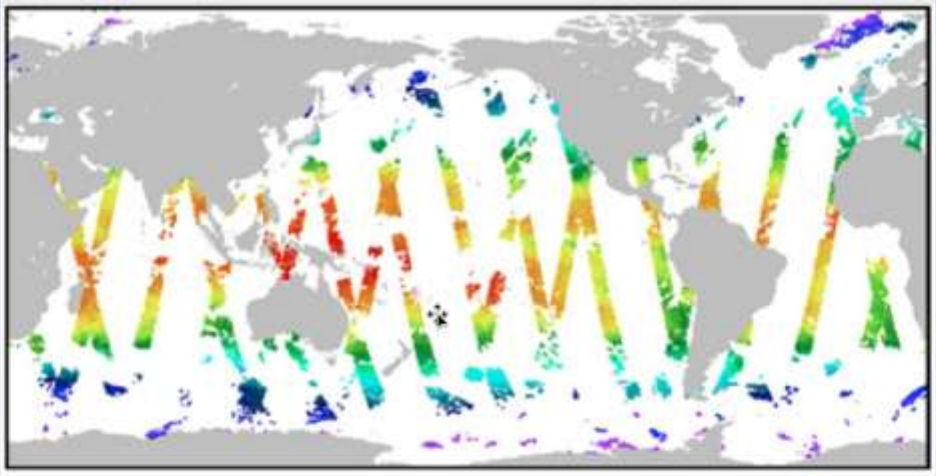

ATSR SST (V2) CLIMATOLOGY

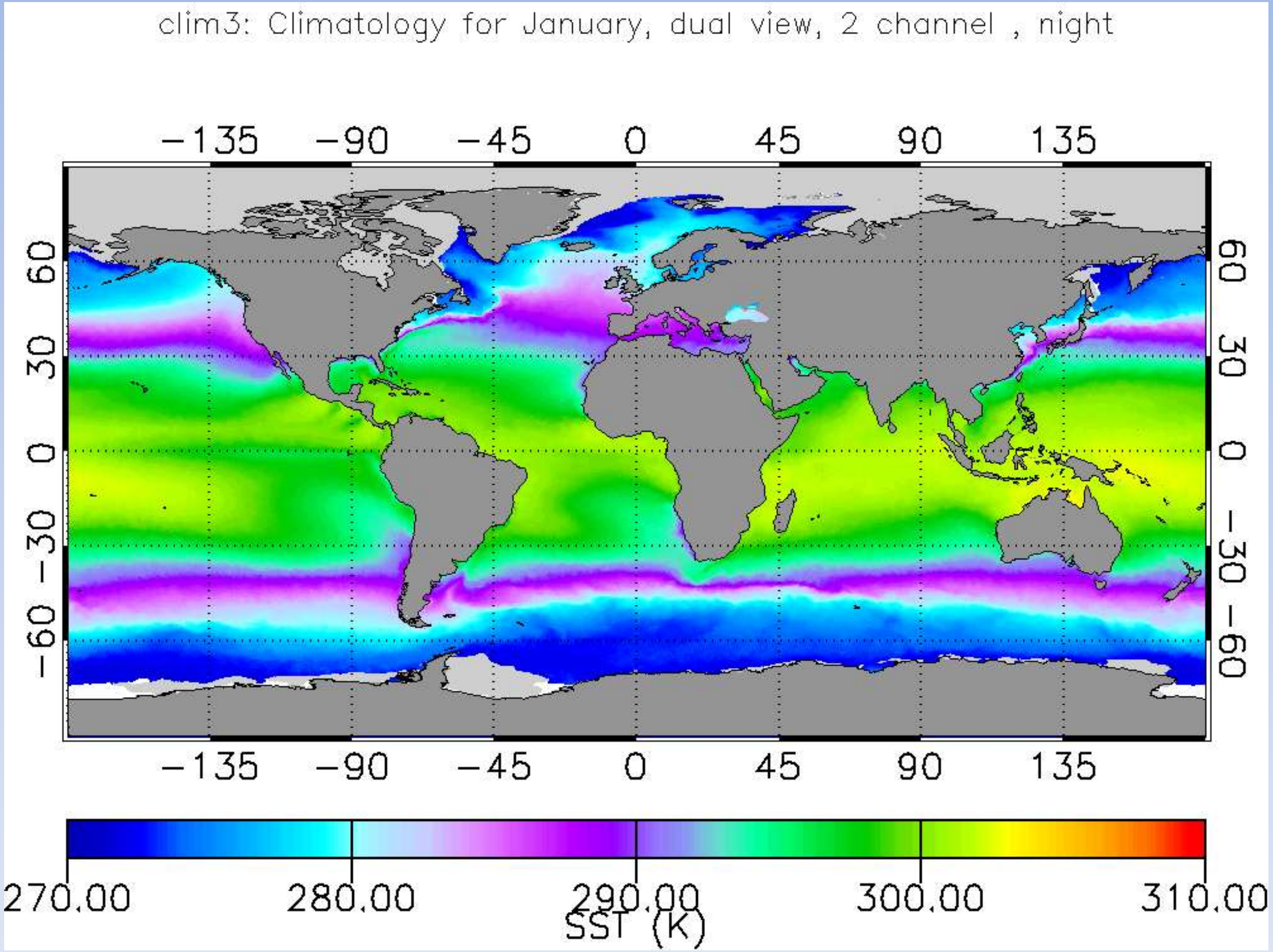

Towards uncertainty schemes

- Building up uncertainties at 10'

Veal et al, 2013

$$\sigma^2_{10', month} = \frac{\sigma^2_{10', day}}{N_{day}} + \sigma^2_{Temp} + \sigma^2_{Adj}.$$

1st term: reduction of random error (0.16 K initially)

2nd term: temporal sampling (SST gradient and time differences)

$$\varepsilon_{Temp} = \overline{\Delta t'} \times \frac{\partial T}{\partial t}.$$

3rd term: alignment of AATSR and ATSR-2

- Aggregating uncertainties at 5° (and similarly to global mean errors)

$$\sigma^2_{5°, month} = \sigma^2_{data} + \sigma^2_{sampling}.$$

Both terms require knowledge of correlations e.g. higher res. uncertainties and spatial sampling

$$\sigma^2_{data} = \frac{1}{N^2}\left[\sum_{i=1}^{N} \sigma_i^2 + \sum_{i=1, i \neq j}^{N} \sum_{j=1, j \neq i}^{N} R_{i,j}\sigma_i\sigma_j\right].$$

University of Leicester

January 2010

MONTHLY SAMPLING ERRORS

Veal et al, 2013

EOS

Uncertainty on monthly average, 10' cell

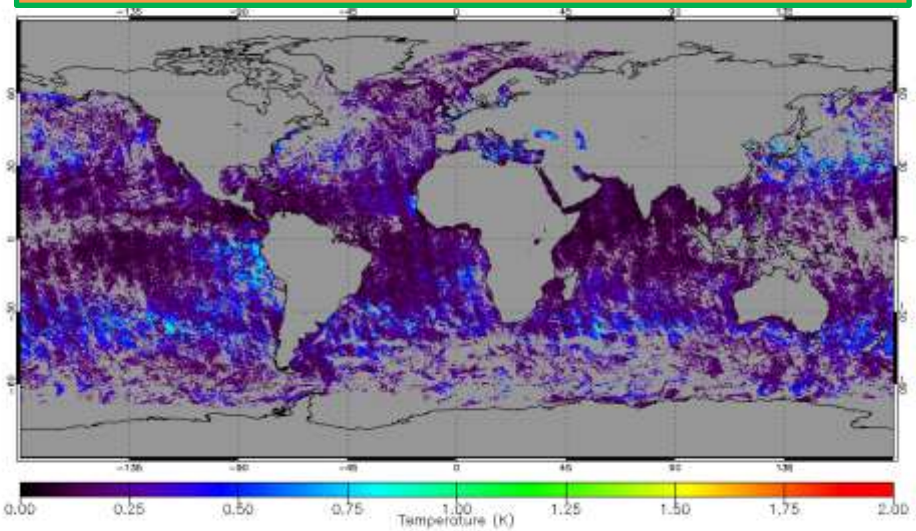

Uncertainty on daily average, 10' cell

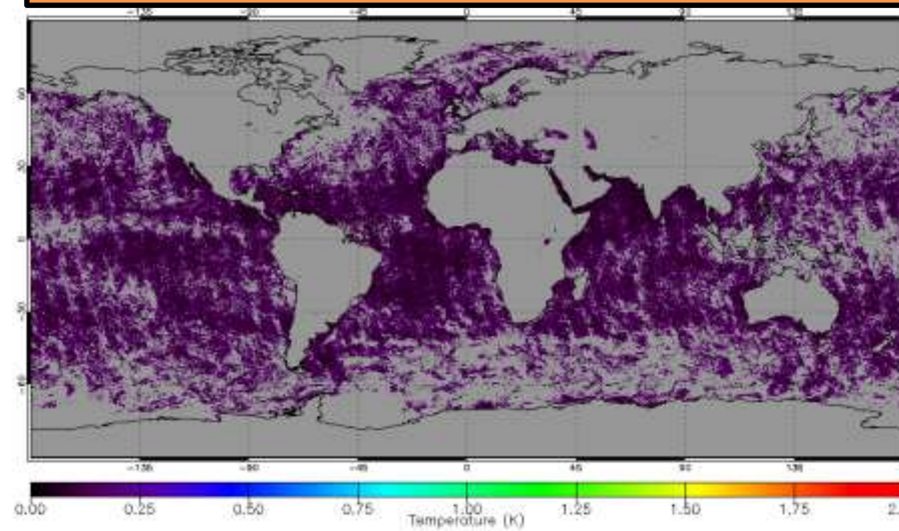

Uncertainty due to temporal sampling

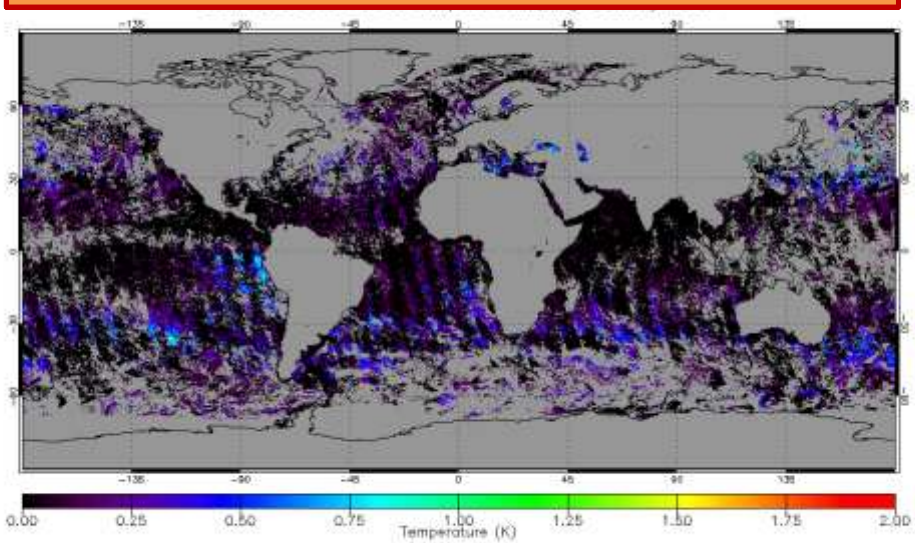

Number of daily samples

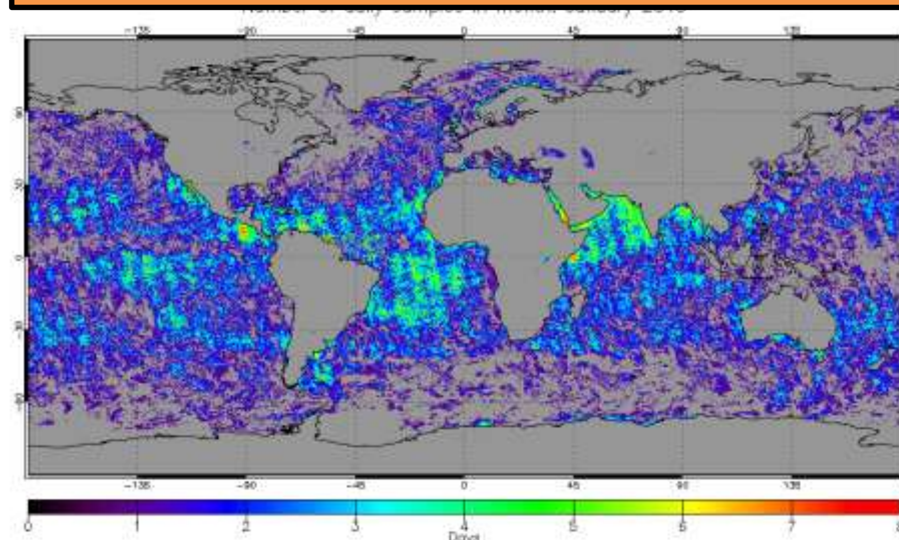

Aggregation/sampling 5°

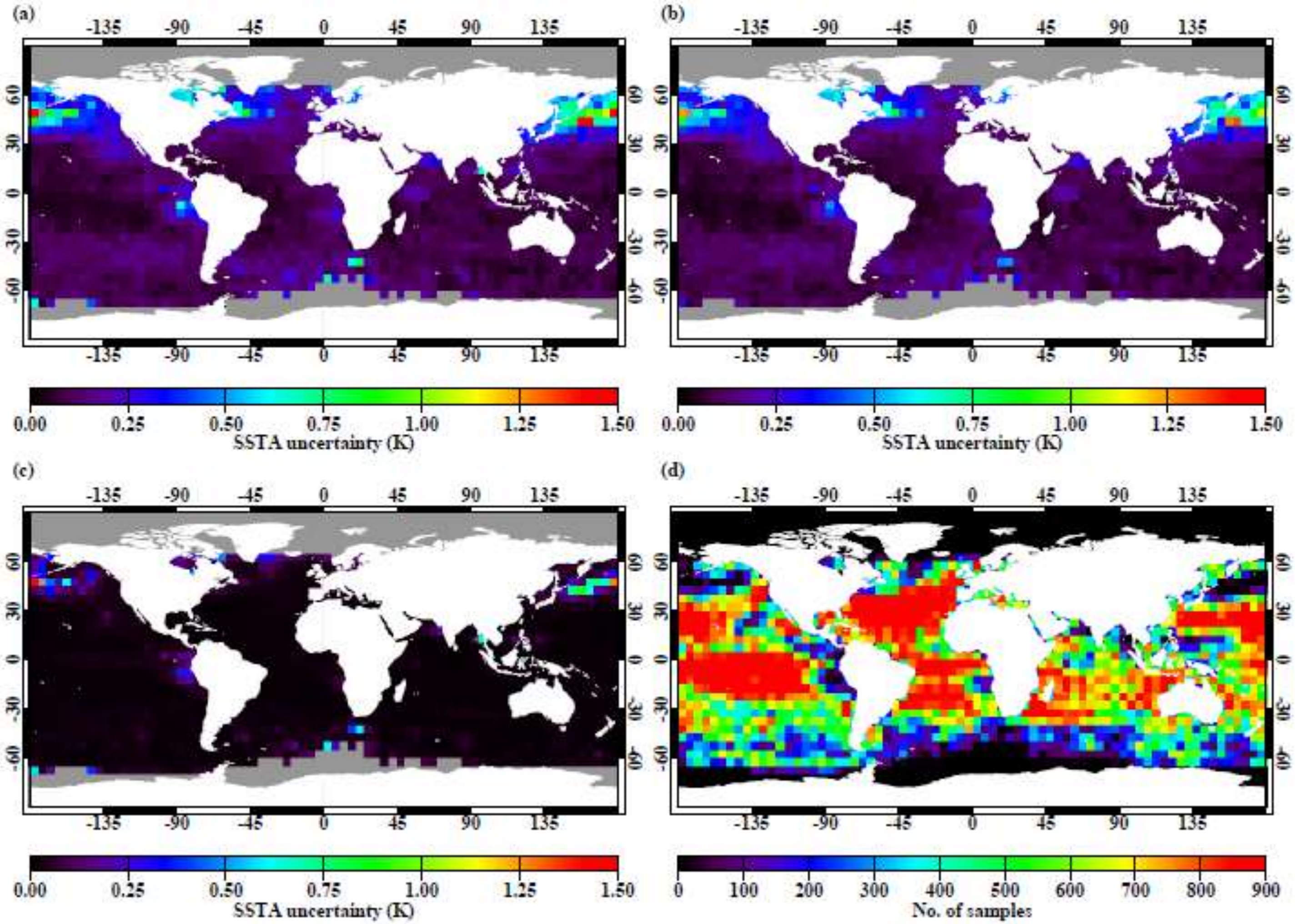

Veal et al, 2013

Figure 9: The 1 sigma uncertainty on the 5° box mean SST anomaly for July 2006 (AATSR) (a) total uncertainty ($\sigma_{5°,month}$) (b) uncertainty due to uncertainties on 10′ cells (σ_{data}) (c) uncertainty due to spatial undersampling ($\sigma_{sampling}$) (d) number of 10′ samples in 5° box (N).

Version 2.0 Nighttime dual-view 3-channel (nD3)

- anomaly to 1997-2011 ATSR nD3 climatology

Uncertainties on global mean anomaly are around 0.014 K for ATSR-2 and 0.011 K for AATSR

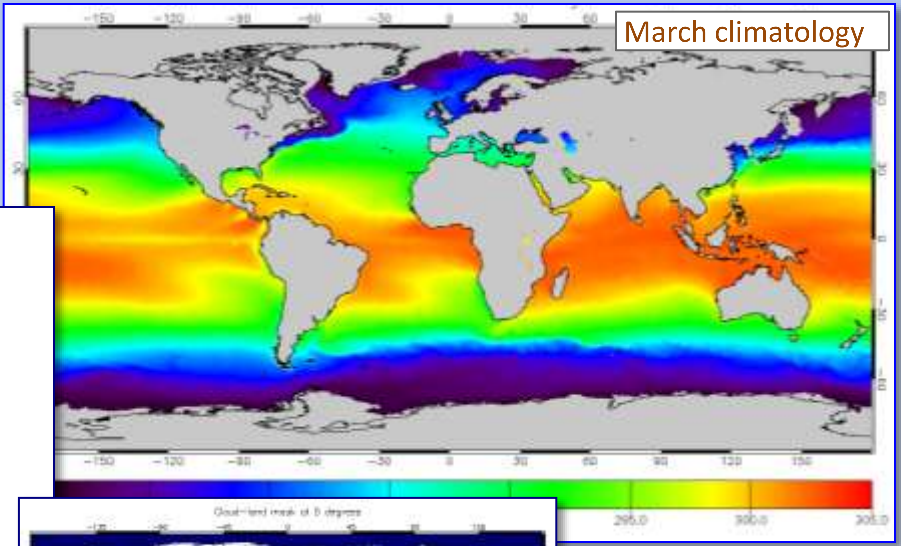

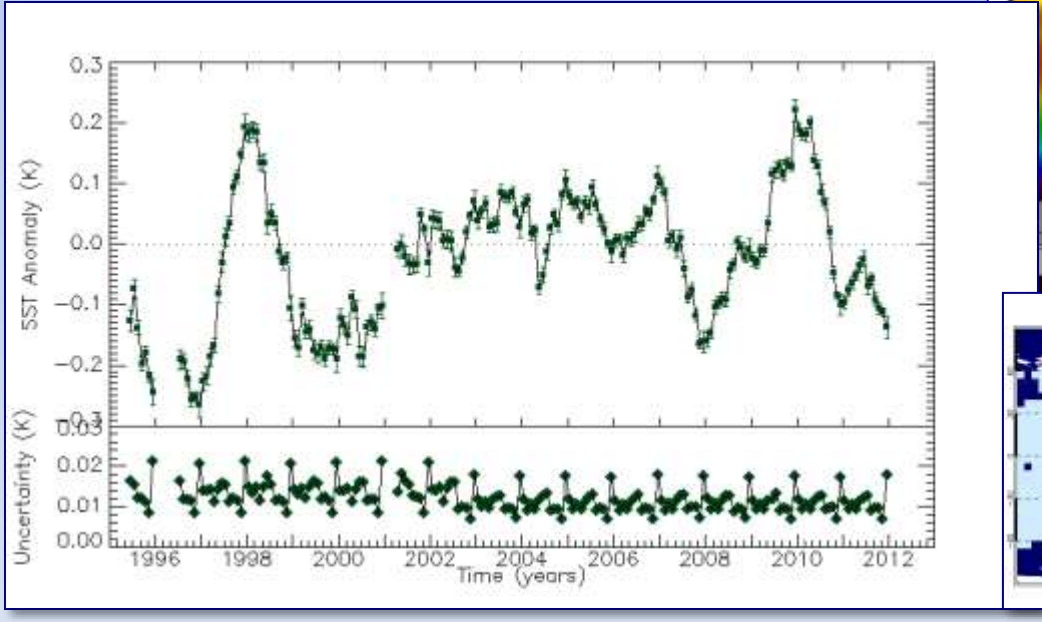

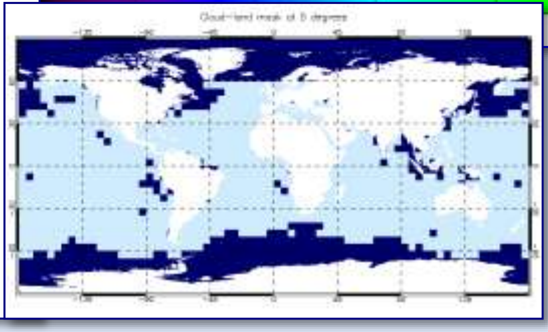

ARC vs ESA V2.0

- ARC = ATSR Re-analysis for climate
- Improved coefficients for retrievals (rad. transfer; simulation profiles; path angle calcs)
- Improved cloud clearing scheme; **algorithm uncertainties**
- **Different homogenisation approach (radiances rather than SSTs)**
- **ATSR-depth calculated for better comparison to in-situ**
- Presented in IPCC 5th Assessment Report

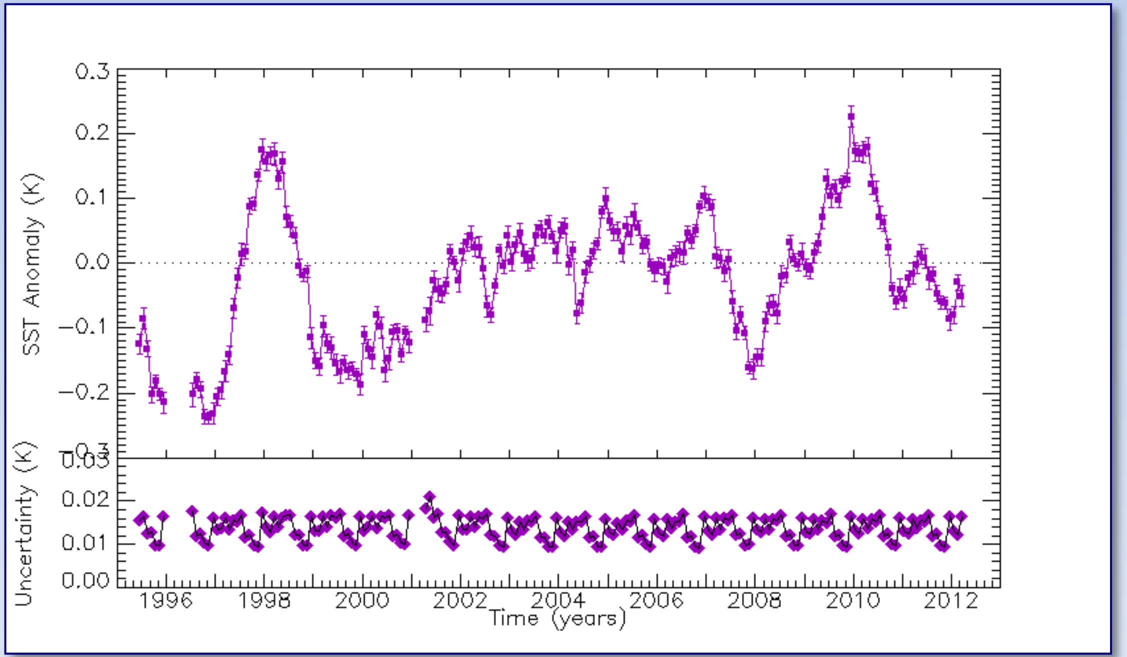

- Embury and Merchant, RSE, 2012
- Embury, Merchant, Corlett, RSE, 2012
- Merchant et al, 2012.

ARC cf. V2: night-time D3 skin

K. Veal

ARC
V2

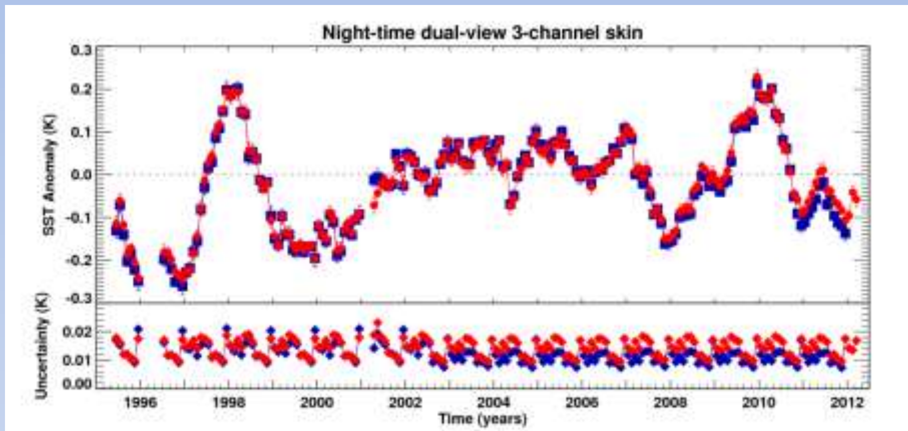

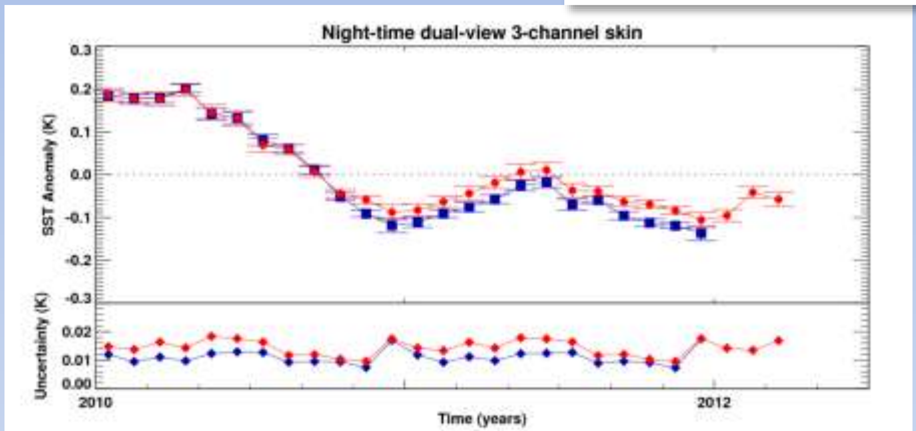

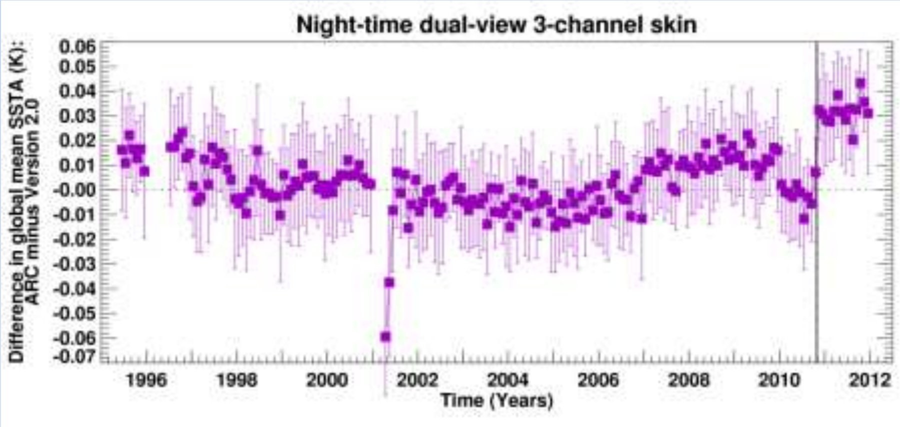

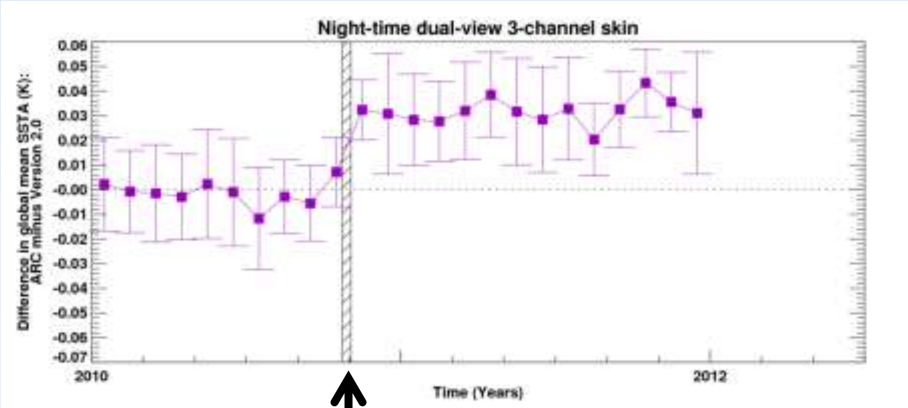

Envisat orbit change

IPCC ATSR SST vs HadSST3

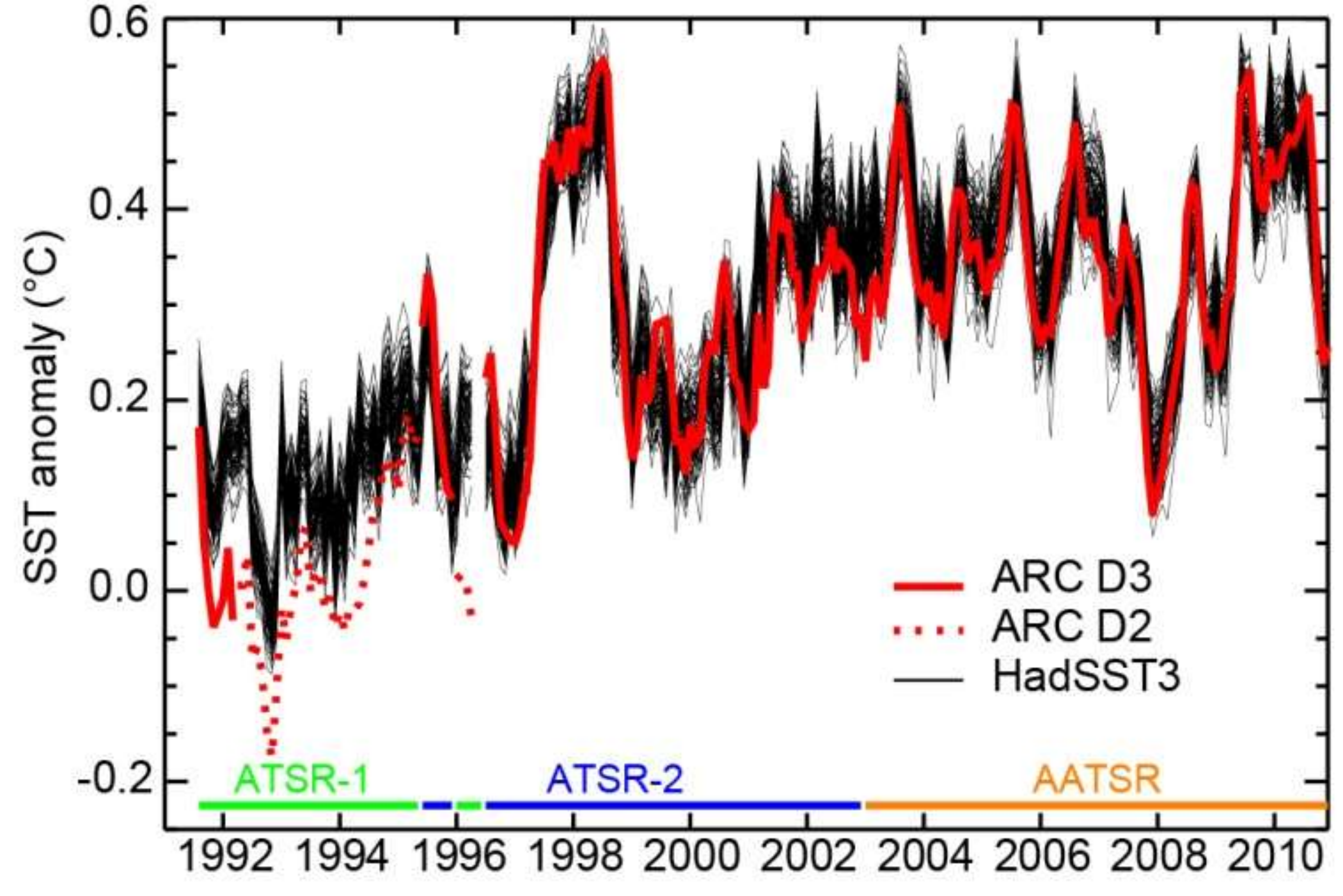

Figure 2.17: Global monthly mean Sea Surface Temperature (SST) anomalies relative to a 1961–1990 climatologyfrom satellites (ATSRs) and in situ records (HadSST3). Black lines: the 100-member HadSST3 ensemble. Red lines: ATSR-based night-time subsurface temperature at 0.2m depth (SST0.2m) estimates from the ATSR Reprocessing for Climate (ARC) project. Retrievals based on three spectral channels (D3, solid line) are more accurate than retrievals based on only two (D2, dotted line). Contributions of the three different ATSR missions to the curve shown are indicated at the bottom. The in situ and satellite records were co-located within 5° × 5° monthly grid boxes: only those where both datasets had data for the same month were used in the comparison. Adapted from Merchant et al. (2012).

ATSR vs HadSST3; details

Global monthly mean SST: ARC 2m depth vs HadSST3 in situ

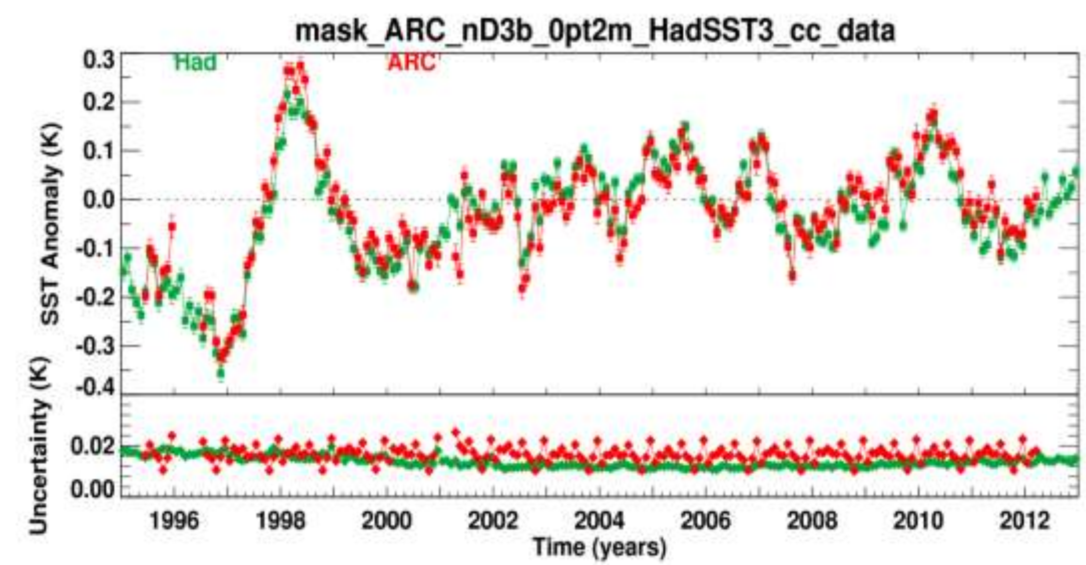

Common sampling area

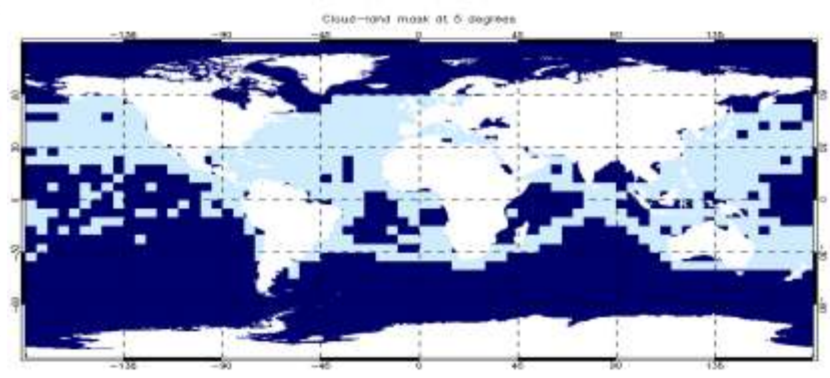

Difference. ARC vs HadSST3 includes 9 month running mean (blue)

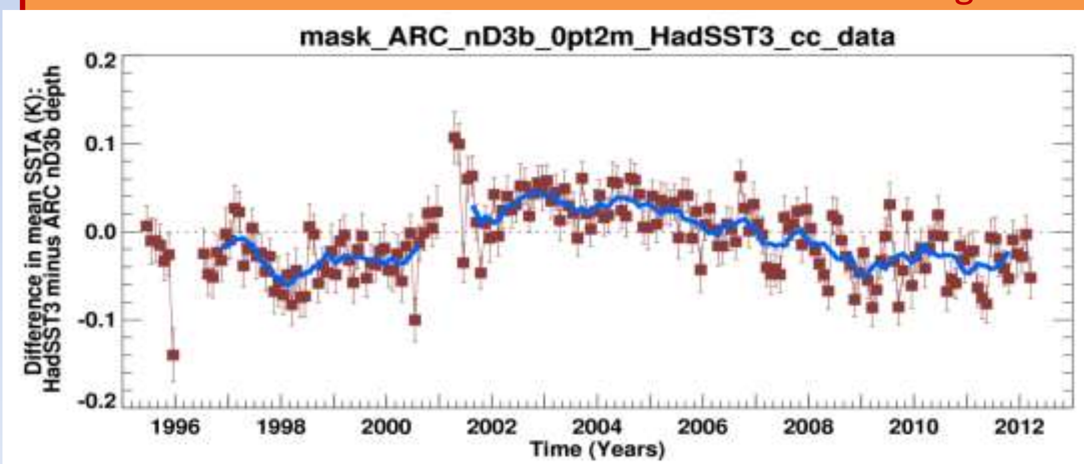

K. Veal

Climate SST

Satellite SST (ATSR) has taught us:

- We can measure climate SST very accurately
- We can impact in situ data, both current and historical.
- There are valid ways to compare to in situ data but need careful thought.
- Crucial factors which needed to be understood:
  - Calibration
  - Validation
  - Climate data as anomalies from mean
  - Aggregation of data
  - Uncertainty estimation
  - Definition of global data and coverage maps.
- Global temperatures are still a hot topic!!

Land Surface Temperatures

Current situation

- Single-sensor LST data-products from satellite have greatly improved:
  - High accuracy of LST data – validation shows majority of biases < 1.0 K (eg Wan & Li, 2008; Coll et al., 2012)
  - Full pixel uncertainty budgets with explicit random, pseudo-random and systematic components following a consistent approach to SST
  - Advances in cloud detection (dynamic probabilistic approaches
- Global LST data which resolve the diurnal cycle will soon be available:
  - Merged geostationary (GEO) and low earth orbit (LEO) data sets will give high spatial resolution, sub-diurnal sampling; estimates of cloud-bias.
- Improved validation protocols are being applied to LST data:
  - Accurate and highly stable in situ instruments; documented calibration at dedicated sites; standardised protocols ; validation of LST uncertainty.
- Increasing confidence in traceability and stability of LST
  - Performance of SST gives confidence In eventual performance of LST

Global time-series of LST

- January to December 2006 [D. Ghent]

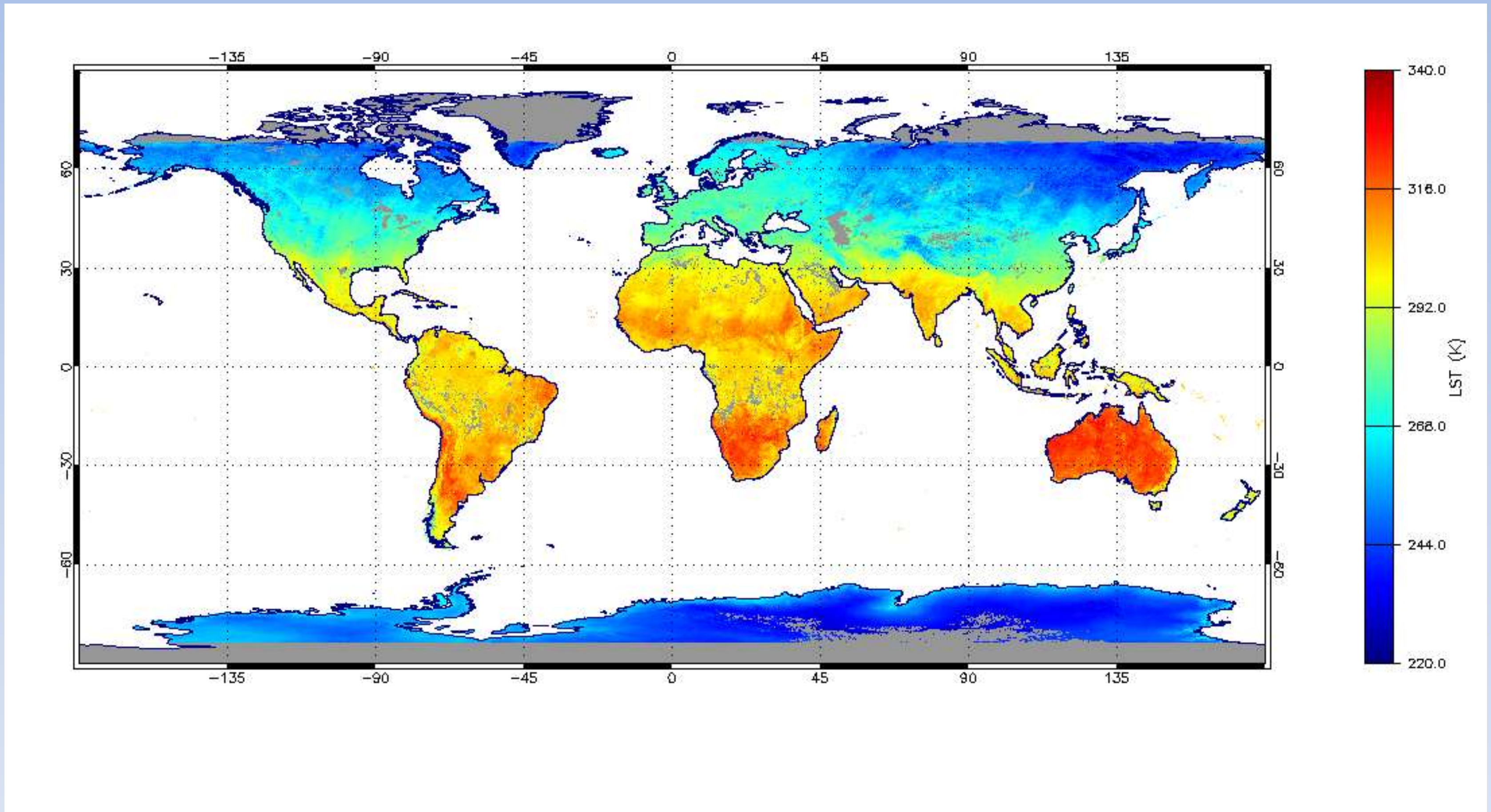

Resolving uncertainty budgets

D. Ghent

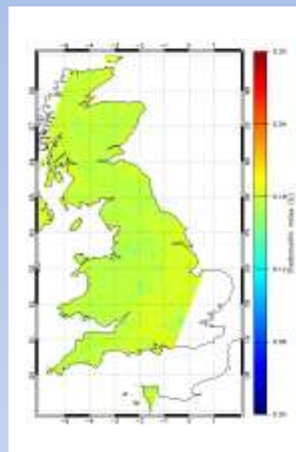

Radiometric noise

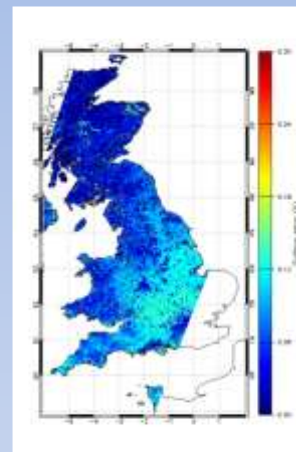

Surface component

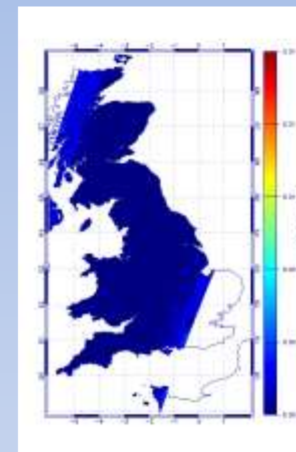

Atmosphere component

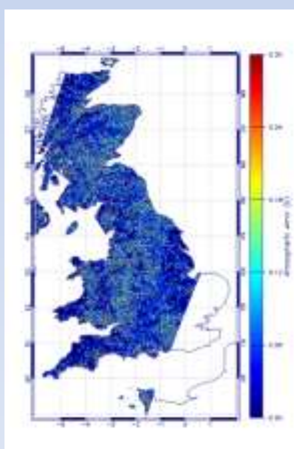

Geolocation

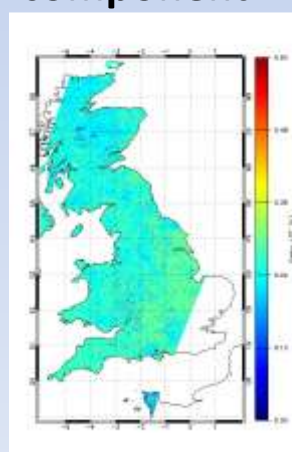

Model fitting

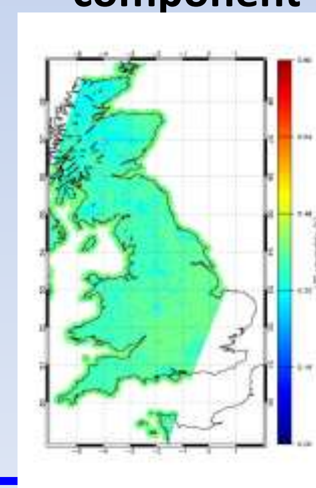

Total

0.8 K

0.4 K

0.0 K

LST Time Series

D. Ghent

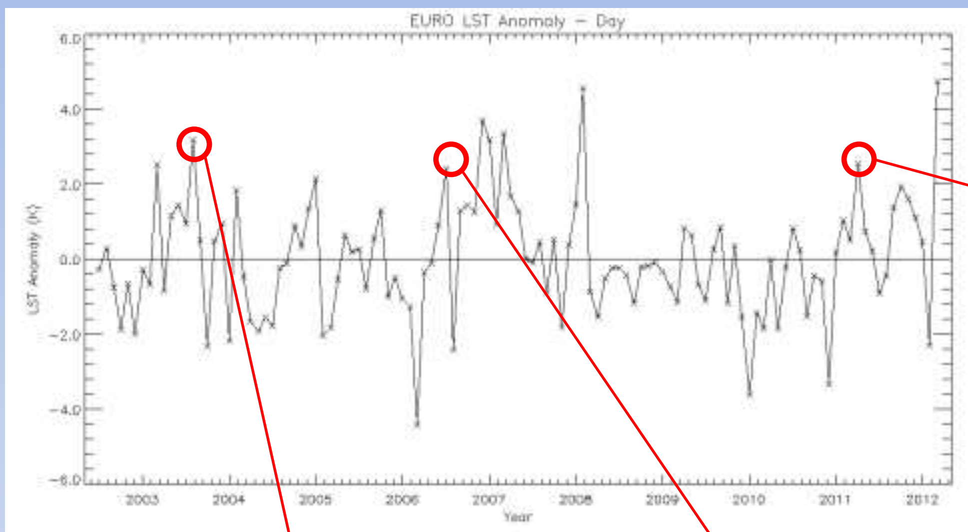

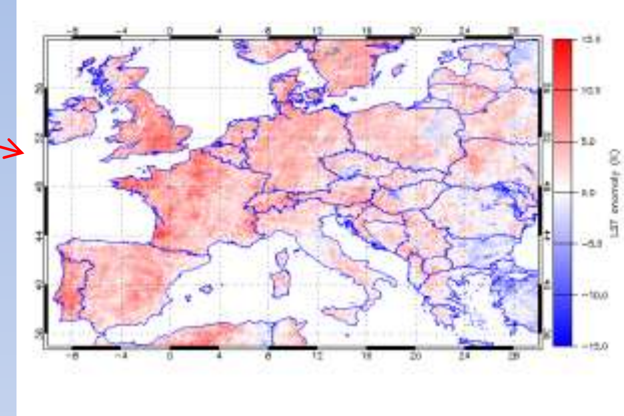

Apr 2011 anomaly

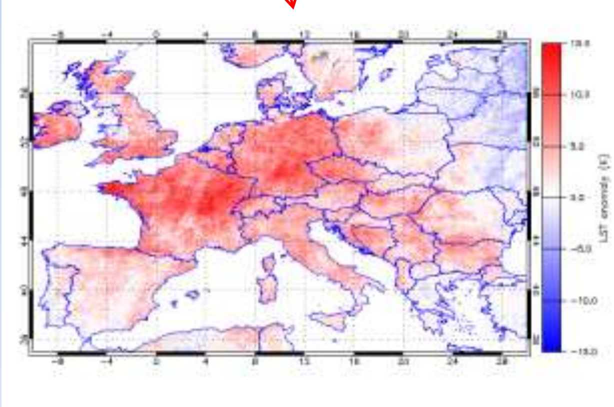

Aug 2003 anomaly

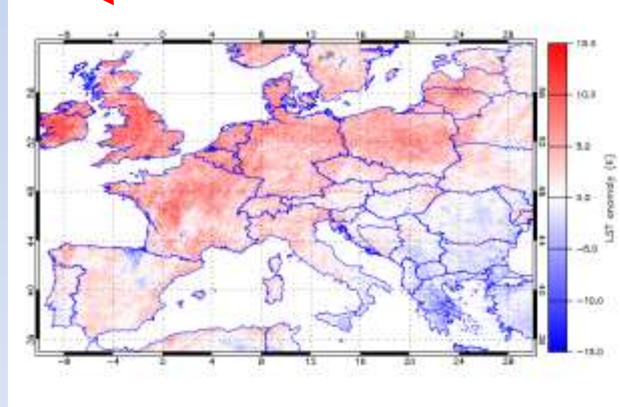

Jul 2006 anomaly

AATSR LST daytime **anomalies** during relative heatwaves

LONDON; M. Perry

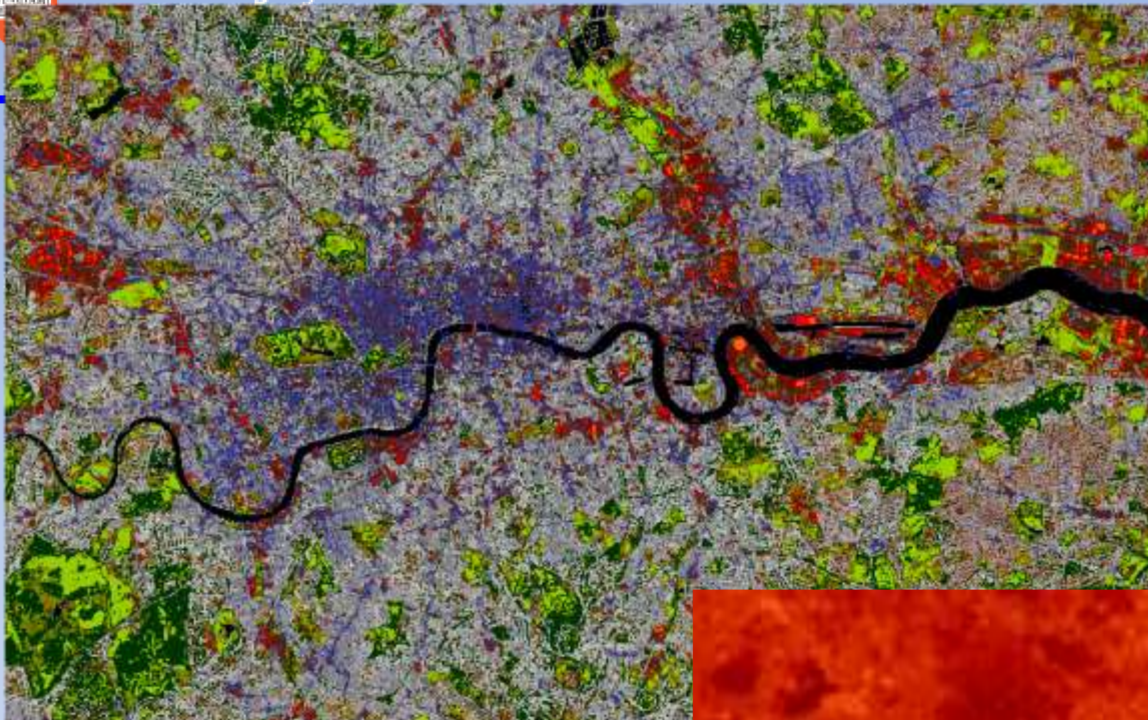

Land classification over central London using k-means cluster analysis of 9 LANDSAT 8 channels. Capable of 30m resolution.

Greens – parks/trees,
Reds – more industrial,
Purple – dense urban/commercial,
Greys - represent different densities of urban/ residential cover.
Black - water

Surface temperature plot over central London using LANDSAT 7 thermal data 90m resolution. LST accuracy limited by a lack of high resolution urban emissivity data.

The future:

Sea and Land Surface Temperature Radiometer

SLSTR characteristics

- Equivalent baseline performance to AATSR (ATSR-4!)
- Backwards oblique view + double scanner
- Wider swath (improved re-visit)
- Recognition of LST in addition to SST

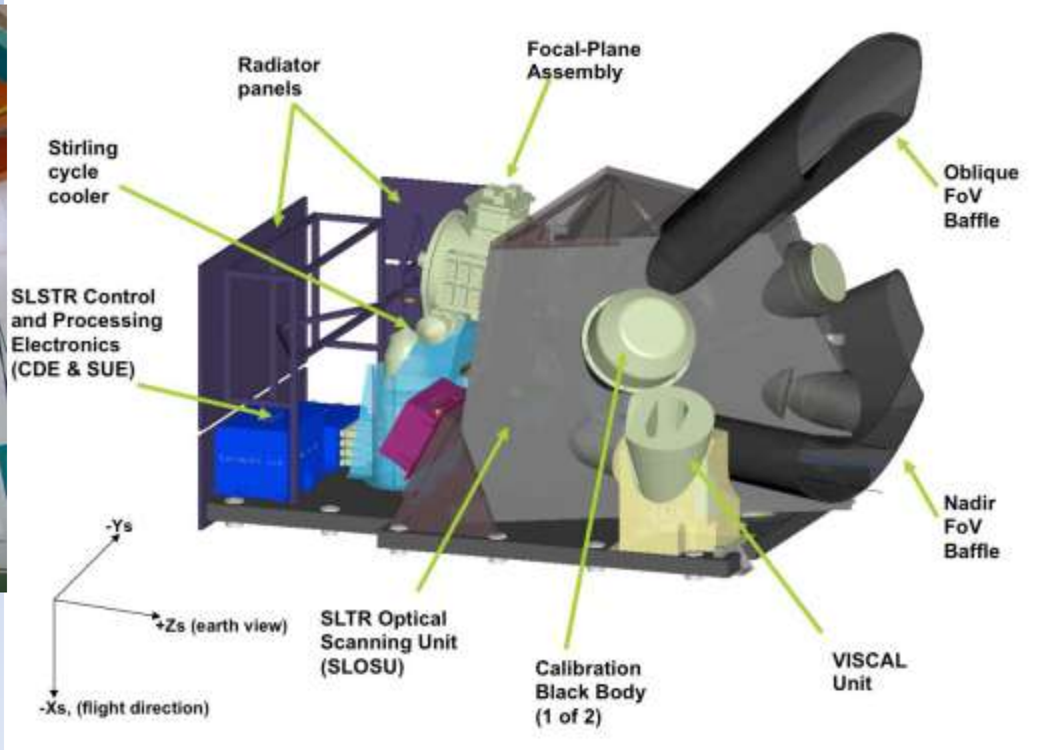

Coppo et al, J. Mod. Opt, 2010
Donlon et al, RSE, 2012

SST COVERAGE IMPROVEMENT

- Lack of samples results in temporal sampling error in climate record monthly mean
- Also indirectly affects estimates of most appropriate temperature gradients
- Improved daily coverage would be a real boost

Daily independent "climate-quality" coverage

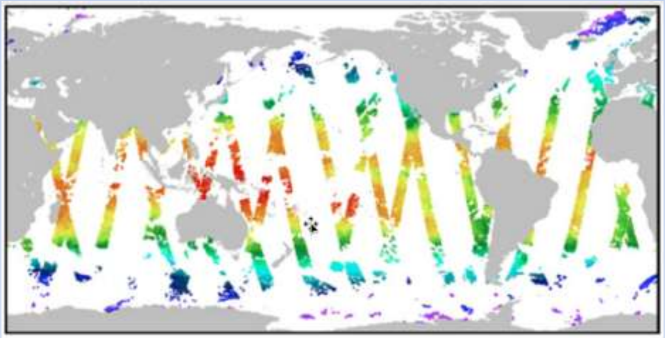

ATSR (ATSR Reprocessing for Climate)

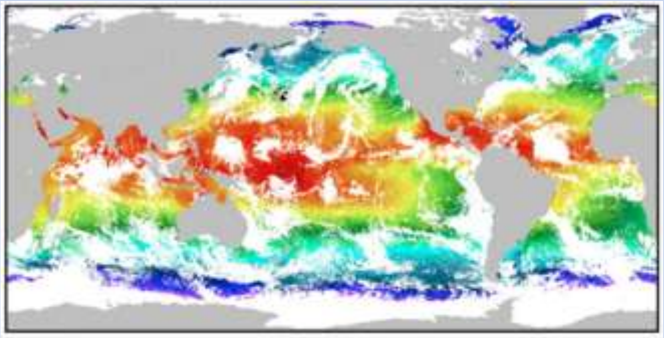

AVHRR (SST CCI)
SLSTR (Sentinel-3

POLAR CHANGE

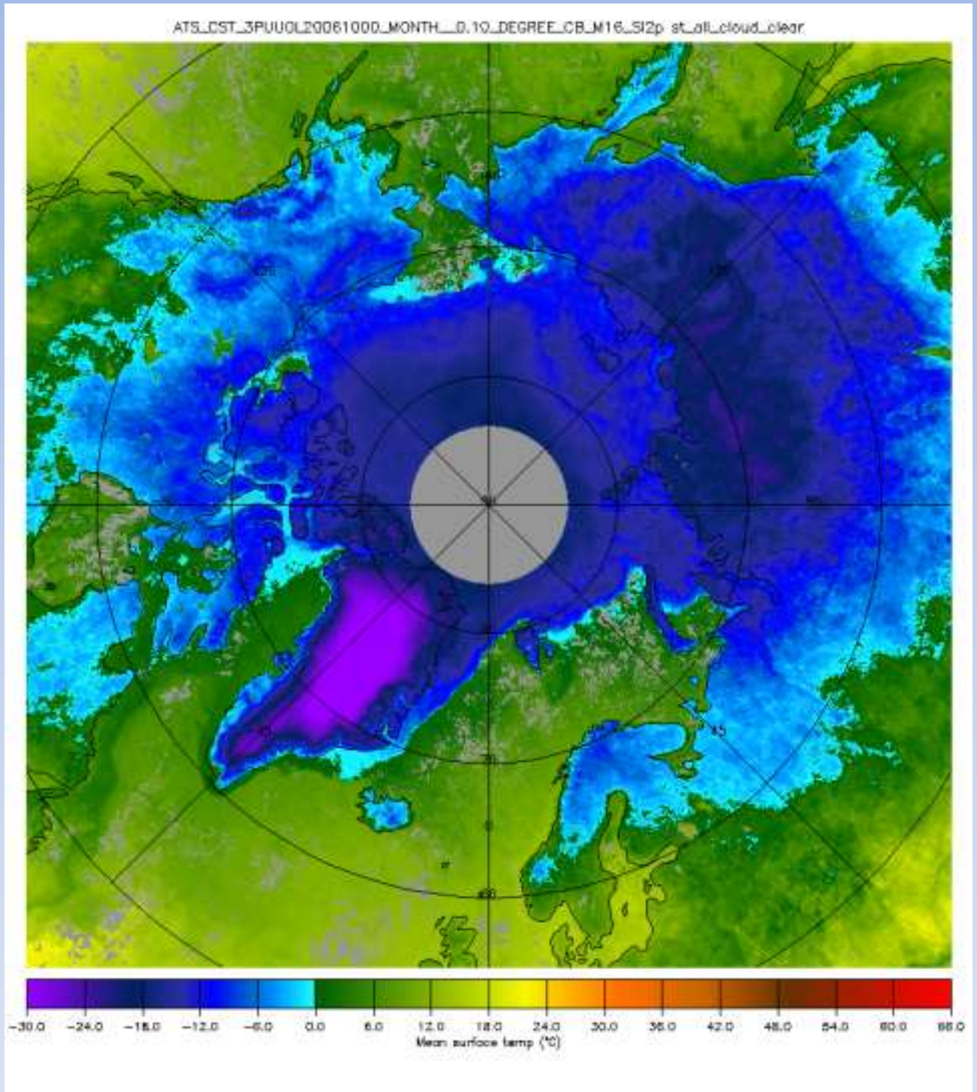

K. Veal

Monthly mean ST for October 2006